

The universal thermodynamic properties of Extremely Compact Objects

Samir D. Mathur¹ and Madhur Mehta²

Department of Physics
The Ohio State University
Columbus, OH 43210, USA

Abstract

An extremely compact object (ECO) is defined as a quantum object without horizon, whose radius is just a small distance s outside its Schwarzschild radius. We show that any ECO of mass M in $d+1$ dimensions with $s \ll (M/m_p)^{2/(d-2)(d+1)}l_p$ must have (at leading order) the same thermodynamic properties — temperature, entropy and radiation rates — as the corresponding semiclassical black hole of mass M . An essential aspect of the argument involves showing that the Tolman-Oppenheimer-Volkoff equation has no consistent solution in the region just outside the ECO surface, unless this region is filled with radiation at the (appropriately blueshifted) Hawking temperature. In string theory it has been found that black hole microstates are fuzzballs — objects with no horizon — which are expected to have a radius that is only a little larger than the horizon radius. Thus the arguments of this paper provide a nice closure to the fuzzball paradigm: the absence of a horizon removes the information paradox, and the thermodynamic properties of the semiclassical hole are nonetheless recovered to an excellent approximation.

¹ email: mathur.16@osu.edu

² email: mehta.493@osu.edu

Contents

1	Introduction	1
1.1	Plan of the paper	3
2	Structure of an ECO	4
2.1	The radius R_{ECO} , and the condition ECO1	4
2.2	Redshift at the ECO surface, and the condition ECO2	6
2.3	Small energy outside the ECO, and the condition ECO3	6
2.4	A relation following from condition ECO1	8
3	The vacuum stress-energy near an ECO	9
3.1	The vacuum stress-tensor near a black hole horizon	9
3.2	The stress tensor near an ECO	10
3.3	The ECO at a general temperature T	13
4	Relating S to T	13
4.1	Relating the entropy S_{ECO} to the temperature	14
4.2	Relating the emission rate Γ_{ECO} to the temperature	14
5	A heuristic argument for the relation $T_{\text{ECO}} \approx T_{\text{H}}$	18
5.1	The energy of radiation near the ECO	18
5.2	An outline of the argument	20
5.2.1	The case $T_{\text{ECO}} < T_{\text{H}}$	20
5.2.2	The case $T_{\text{ECO}} > T_{\text{H}}$	21
5.3	Defining a useful scale Δr_{crit}	23
5.4	The argument for $T_{\text{ECO}} < T_{\text{H}}$	23
5.5	The estimate for $T_{\text{ECO}} > T_{\text{H}}$	24
6	Using the Tolman-Oppenheimer-Volkoff equation	26
6.1	Approximating the TOV equation	27
6.1.1	Preliminary steps	28
6.1.2	Approximating the TOV equation	29
6.1.3	Solving the approximate TOV equation	30
6.1.4	Range of validity of the approximation	31
6.2	Analyzing the approximate TOV solution	32
6.2.1	The case $C_3 > 0$, $r_1 < R_{\text{ECO}}$	33
6.2.2	The case $C_3 < 0$, $r_1 > R_{\text{ECO}}$	33
6.3	Checking the consistency of condition ECO3	35
6.4	Summary	36
7	An ECO in 1+1 dimensional dilaton gravity	37
7.1	The model	37
7.2	Solving the equations	38
7.3	Finding the Boulware and Hartle-Hawking states	40
7.4	Analysis of the solution	41
7.4.1	$T_{\text{ECO}} < T_{\text{H}}$	41
7.4.2	$T_{\text{ECO}} > T_{\text{H}}$	42
7.5	The form of the stress tensor	44
8	Discussion	45

1 Introduction

Consider a ball of steel with mass M . This mass does not determine the temperature T of the ball; we can choose different values of the temperature, including $T = 0$. There is also no simple relation between the mass M and the entropy S of the ball; this entropy depends on the detailed composition of the ball. Even if we know M, T, S , we cannot predict the radiation rate Γ from the ball; this radiation rate depends on the surface area and shape of the ball.

Remarkably, the situation is much simpler for black holes. Consider the Schwarzschild hole in $3 + 1$ dimensional spacetime. Hawking [1] found that the temperature of the hole is

$$T_H = \frac{1}{8\pi GM}. \quad (1.1)$$

The entropy is [1, 2]

$$S_{bek} = \frac{A}{4G}, \quad (1.2)$$

where A is the surface area of the horizon. Hawking found that the hole radiates ‘thermally’ in the sense that the radiation rate is related to the absorption cross section in the manner expected from detailed balance. Thus consider the radiation of a massless scalar field. Then the number of particles emitted per unit time in the energy range $d\omega$ is $\Gamma_H[l, m, \omega] \frac{d\omega}{2\pi}$ with

$$\Gamma_H[l, m, \omega] = \frac{\mathcal{P}[l, m, \omega]}{e^{\frac{\omega}{T_H}} - 1}, \quad (1.3)$$

where $\mathcal{P}[l, m, \omega]$ is the absorption probability for an incoming spherical wave of energy ω in the spherical harmonic $Y_{l,m}$.

Thus, the thermodynamical properties of the Schwarzschild hole are determined completely by the mass M of the hole. More generally, the thermodynamical properties of the hole are determined by the conserved quantum numbers characterizing the hole—the mass M , the charges Q_i and the angular momenta J_i . What is the reason for this very special behavior of black holes?

The universal thermodynamical behavior of black holes is often attributed to the presence of a *horizon* in the black hole geometry. Bekenstein’s argument for entropy [2] started with the idea that the entropy of matter falling through a horizon is ‘lost’ to the outside world; to prevent a violation of the second law of thermodynamics one must then attribute an entropy to the hole, which ends up taking the value (1.2). One would not make such an argument for the entropy of matter falling into a normal box, since we would not think of this entropy as having been ‘lost’; thus the existence of a horizon was important to the argument. Similarly, Hawking’s computation of radiation from the hole, which leads to the relations (1.1) and (1.3), involves the horizon in fundamental way. Outgoing null geodesics in the vicinity of the horizon separate: the ones just outside the horizon ultimately escape to infinity, while those just inside the horizon fall into the singularity. This separation leads to a stretching of spacelike slices in the black hole geometry, and the consequent production of particle pairs around the horizon. One member of the pair (which we call b) escapes to infinity as ‘Hawking radiation’, while the other member (which we call c) falls into the hole with negative energy and thus lowers the mass of the hole. The above observations indeed suggest that there is a close relation between the existence of a horizon and the emergence of black hole thermodynamics (1.1)-(1.3). There

have been attempts to relate the fact that a horizon ‘traps information inside’ to the notion that entropy is a ‘lack of information’.

But this traditional picture of the hole possessing a horizon leads to a serious problem—the information paradox [1, 3]. The (b, c) quanta of the Hawking pair are in an entangled state, which can be schematically written as

$$|\psi\rangle_{pair} = \frac{1}{\sqrt{2}} (|0\rangle_b |0\rangle_c + |1\rangle_b |1\rangle_c) . \quad (1.4)$$

Thus we get a monotonically rising entanglement between the emitted radiation and the remaining hole, leading to a sharp puzzle near the endpoint of evaporation. If the hole evaporates away completely, then the radiation is left in an entangled state, but there is nothing that it is entangled *with*; such radiation cannot be described by any quantum state, leading to a violation of quantum unitarity. If the evaporation terminates in a planck sized remnant, then we face difficulties with a planck size object having an unbounded number of internal states. The small corrections theorem [4] shows that Hawking’s argument is stable against any small correction to the horizon dynamics; we cannot escape the problem of monotonically rising entanglement by seeking subtle correlations among the large number of radiated quanta.

String theory computations suggest that the microstates of the black hole are horizon sized quantum objects called *fuzzballs* [5–14]. A fuzzball does not have a horizon and radiates from its surface like any other normal body; thus there is no information paradox. An entropic argument indicates that the surface of a generic fuzzball should be at a proper distance $s \sim l_p$ outside the Schwarzschild radius r_0 of the semiclassical hole [15]. Thus fuzzballs are expected to be extremely compact. In what follows we will use the term ECO to represent any ‘Extremely Compact Object’; i.e., an object with no horizon and a radius which is just a little larger than the horizon radius r_0 for its mass M .

In this paper we will argue that any Extremely Compact Object (ECO) will have the *same* thermodynamical properties (1.1)–(1.3), as the semiclassical black hole, to leading order. For $d+1$ dimensions, our arguments will hold for ECOs whose surface is at a proper distance

$$s_{\text{ECO}} \ll \left(\frac{M}{m_p} \right)^{\frac{2}{(d-2)(d+1)}} l_p , \quad (1.5)$$

outside the horizon radius r_0 . For $3+1$ dimensions, this is

$$s_{\text{ECO}} \ll \left(\frac{M}{m_p} \right)^{\frac{1}{2}} l_p . \quad (1.6)$$

The deviations of the thermodynamics parameters of the ECO from the corresponding values of the black hole become smaller as s is made smaller. The essence of the argument will rely on looking at the quantum stress tensor just outside the surface of the ECO (a brief version of this argument was presented in the essay [16]).

Before proceeding with our analysis, we note a result obtained in [17, 18]. Suppose the black hole is replaced by a thin spherical shell which is supported by its own pressure, and stands a small distance outside its horizon radius. It was argued that such a shell will have to be in equilibrium with the local Unruh radiation, and that this fact leads to the entropy (1.2) for the shell. This shell thus gives a ‘brick wall’ type of model [19] for a black hole, which is at

the standard black hole temperature T_H . In the present paper, our interest is in the converse question: can there be an ECO whose temperature T_{ECO} is *different* from T_H ? We will consider a general ECO, rather than any particular model like a thin shell. Thus our arguments will proceed on somewhat different lines from the arguments of [17], and will not involve the internal structure of the ECO at all. But like [17] we will also use the fact that the near-surface region of an ECO has a negative vacuum energy, equal in magnitude to the energy of Unruh radiation near a black hole horizon.

We also note that many aspects of compact objects have been studied in [20–24].

1.1 Plan of the paper

The plan of this paper is as follows:

- (i) In section 2 we describe the structure of an ECO, and state conditions ECO1-ECO3 which will define an ECO.
- (ii) In section 3 we note that the vacuum state near the surface of an ECO has a negative energy density, which (to leading order) is the same as the negative energy density of the Boulware vacuum.
- (iii) In section 4 we note that if the ECO had the same temperature $T_{\text{ECO}}(M)$ as the temperature $T_H(M)$ for a black hole then we will also have an agreement of entropies $S_{\text{ECO}}(M) = S_{\text{bek}}(M)$; this just follows from the laws of statistical mechanics valid for systems with many degrees of freedom. We then show that if $T_{\text{ECO}} = T_H$, then the radiation rate from the ECO, $\Gamma_{\text{ECO}}[\{l\}, \omega]$, will also be equal (to leading order) to the radiation rate from the black hole, $\Gamma_H[\{l\}, \omega]$. This argument relies on the extreme compactness of the ECO.
- (iv) In section 5 we give a heuristic derivation of the result that the temperature of an ECO must equal the temperature of the black hole. The arguments will be rough but they nonetheless capture the essential physics of the problem and lead to the scale (1.5) for compactness of an ECO.
- (v) In section 6 we will make a plausible assumption about the stress tensor describing the vacuum near the ECO surface, and solve the Tolman-Oppenheimer-Volkoff (TOV) equation in a near-surface approximation. We will find that if the ECO satisfies our conditions ECO1-ECO3, then there is no consistent solution to this equation if $T_{\text{ECO}} \neq T_H$.
- (vi) In section 7 we consider $1 + 1$ dimensional dilaton gravity coupled to minimal scalars. This case was analyzed in detail in [25], and we will recall their results. In this analysis the stress tensor of the vacuum is taken into account exactly, since it can be computed from the conformal anomaly. We note similarities and differences between this $1 + 1$ dimensional case and the behavior in higher dimensions.
- (vii) Section 8 is a summary and discussion.

2 Structure of an ECO

In this section we will describe the structure of what we mean by an Extremely Compact Object (ECO). While describing this structure we will extract properties ECO1-ECO3 which will define our ECO.

We will assume for simplicity that the ECO is spherically symmetric to leading order. Thus while the interior of the ECO can have structures at microscopic scales that are not spherically symmetric, we will assume that the gravitational properties of the ECO in the region outside the ECO are well approximated by a spherically symmetric and time-independent configuration. The ECO is described by a mass M measured at infinity, and has vanishing angular momentum and charge.

The number of space dimensions will be called d . We define the planck length as

$$G = l_p^{d-1}, \quad (2.1)$$

and the planck mass as

$$m_p = \frac{1}{l_p}. \quad (2.2)$$

We will assume that the mass M of the ECO satisfies

$$\frac{M}{m_p} \gg 1. \quad (2.3)$$

2.1 The radius R_{ECO} , and the condition ECO1

Our Extremely Compact Object should be characterized by a radius R_{ECO} that is just a little larger than the horizon radius for a black hole of mass M . In such a situation, the surface of the ECO feels a strong inward pull of gravity, and for simple distributions of matter, an equilibrium solution is not possible. For example the Buchdahl theorem [26] in 3+1 dimensions says that a spherically symmetric ball of perfect fluid (with pressure decreasing outwards) cannot resist collapse if its radius is less than $\frac{9}{4}GM$. In string theory, it was noted in [27] how fuzzballs evade such a conclusion because the compact dimensions are not trivially tensored with the noncompact ones. Recently, string theory constructions have been given for solitonic stars; formally these structures can be extrapolated to a point where they are only slightly larger than their Schwarzschild radius [28–32].

Our ECO will be described by a radius $r = R_{\text{ECO}}$. Here the coordinate r is defined in the usual way as the radius where the area of the angular sphere is $4\pi r^2$ in 3+1 dimensions, and $r^2\Omega_{d-1}$ in $d+1$ dimensions. We will make no assumptions about the structure in the region $r < R_{\text{ECO}}$; this can be a region with significant quantum gravitational effects, so that spacetime itself may not make sense here. But in the region $r > R_{\text{ECO}}$ we require usual semiclassical dynamics to hold to sufficient accuracy for all our purposes. In the semiclassical region $r > R_{\text{ECO}}$ we take the metric ansatz in $d+1$ spacetime dimensions

$$ds^2 = -e^{2\alpha(r)}dt^2 + e^{2\beta(r)}dr^2 + r^2d\Omega_{d-1}^2. \quad (2.4)$$

The Einstein equations $G_{\mu\nu} = 8\pi GT_{\mu\nu}$ have the vacuum Schwarzschild solution in 3+1 dimensions

$$ds^2 = -\left(1 - \frac{2GM}{r}\right)dt^2 + \frac{dr^2}{1 - \frac{2GM}{r}} + r^2d\Omega_2^2. \quad (2.5)$$

For $d+1$ dimensions the vacuum Schwarzschild solution is

$$ds^2 = - \left(1 - \frac{r_0^{d-2}}{r^{d-2}} \right) dt^2 + \frac{dr^2}{1 - \frac{r_0^{d-2}}{r^{d-2}}} + r^2 d\Omega_{d-1}^2, \quad (2.6)$$

where

$$r_0^{d-2} = \mu GM, \quad \mu = \frac{16\pi}{(d-1)\Omega_{d-1}}. \quad (2.7)$$

Here and in all later equations, when we talk of a general space-time dimension $d+1$, we have in mind $d \geq 3$. In $2+1$ dimensional gravity the mass M does not generate an asymptotically flat spacetime, and we will not consider this case here. The case of $1+1$ dimensional dilaton gravity will be considered separately in section 7; this case allows for a more explicit solution than is possible in higher dimensions.

The requirement that the ECO be extremely compact says that R_{ECO} should be only a little larger than the horizon radius for the same mass M . For the black hole metric (2.6), we can describe the near-horizon region using Rindler coordinates. We define

$$\tilde{t} = \frac{(d-2)}{2r_0} t, \quad s = 2 \left(\frac{r_0(r-r_0)}{d-2} \right)^{\frac{1}{2}}. \quad (2.8)$$

The near-horizon geometry then becomes Rindler space

$$ds^2 \approx -s^2 d\tilde{t}^2 + ds^2 + dx_1^2 + \cdots + dx_{d-1}^2, \quad (2.9)$$

with $x_1 \dots x_{d-1}$ describing the tangent space to the angular sphere.

It is convenient to recast the compactness requirement on R_{ECO} as follows. The horizon radius for a black hole of mass M is $r = r_0$. Let s_{ECO} be the proper distance, measured radially, between a sphere with radius $r = r_0$ and a sphere with radius $r = R_{\text{ECO}}$, in the black hole metric (2.6). From (2.8) we see that

$$s_{\text{ECO}} = 2 \left(\frac{r_0(R_{\text{ECO}} - r_0)}{d-2} \right)^{\frac{1}{2}}. \quad (2.10)$$

An ECO should be characterized by $s_{\text{ECO}} \ll r_0$. For fuzzballs, entropic arguments indicate that $s_{\text{ECO}} \sim l_p$. The arguments of the present paper will hold for a larger range of s_{ECO} (1.5); this range will emerge in the course of our analysis. Note that in defining s_{ECO} we use the black hole metric (2.6) only as a convenient tool to describe the difference between the radius values $r = R_{\text{ECO}}$ and $r = r_0$; the actual metric in the region around $r = R_{\text{ECO}}$ can be very different from the vacuum black hole solution.

We summarize the above discussion in the following property of the ECO:

ECO1: Semiclassical physics holds outside the radius $r = R_{\text{ECO}}$, and this radius R_{ECO} is close to the horizon radius r_0 , with

$$s_{\text{ECO}} \ll \left(\frac{M}{m_p} \right)^{\frac{2}{(d-2)(d+1)}} l_p. \quad (2.11)$$

We can think of (2.11) as describing the ‘compactness’ of an ECO. In what follows we will sometimes refer to the scale

$$s_c \sim \left(\frac{M}{m_p} \right)^{\frac{2}{(d-2)(d+1)}} l_p \sim \left(\frac{r_0}{l_p} \right)^{\frac{2}{d+1}} l_p, \quad (2.12)$$

as the compactness scale.

2.2 Redshift at the ECO surface, and the condition ECO2

The essential property of a black hole is the infinite redshift that we get at the black hole horizon. Any extremely compact object that replaces a black hole should be characterized by a very large (though not infinite) redshift at its surface R_{ECO} . Let us note what the scale of this redshift should be.

We define the redshift parameter $q(r)$ by

$$q(r) \equiv (-g_{tt}(r))^{-\frac{1}{2}}. \quad (2.13)$$

In the Rindler region $(r - r_0)/r_0 \ll 1$, for the black hole metric (2.6), we have

$$q(r) \approx \left(\frac{(d-2)(r-r_0)}{r_0} \right)^{-\frac{1}{2}} \approx \frac{2r_0}{(d-2)s}. \quad (2.14)$$

At the compactness scale s_c (eq.(2.12)), this redshift parameter is

$$q(s_c) \sim \left(\frac{M}{m_p} \right)^{-\frac{2}{(d-2)(d+1)}} \frac{r_0}{l_p} \sim \left(\frac{r_0}{l_p} \right)^{\frac{d-1}{d+1}} \sim \left(\frac{M}{m_p} \right)^{\frac{(d-1)}{(d-2)(d+1)}}. \quad (2.15)$$

Since the ECO is required to have $s_{\text{ECO}} \ll s_c$, we place the following requirement on our ECO:

ECO2: The redshift at $r = R_{\text{ECO}}$ satisfies

$$q(R_{\text{ECO}}) \gg \left(\frac{r_0}{l_p} \right)^{\frac{d-1}{d+1}} \sim \left(\frac{M}{m_p} \right)^{\frac{(d-1)}{(d-2)(d+1)}}. \quad (2.16)$$

2.3 Small energy outside the ECO, and the condition ECO3

It may appear reasonable to require that the spacetime in the region $r > R_{\text{ECO}}$ has zero stress-energy and thus a metric of the black hole form (2.6). But the ECO has in general a nonzero temperature T_{ECO} , and radiation corresponding to this temperature will fill up the region near the ECO. We have in mind temperatures of order the Hawking temperature (1.1), and it is true that the radiation energy density at this temperature is very small at $r \gg R_{\text{ECO}}$. But the energy density of this radiation can be very large close to R_{ECO} due to the large redshift in this region, and contribute a total mass that is $O(M)$. Thus we have to consider the more general ansatz (2.4) for the metric in the region just outside $r = R_{\text{ECO}}$.

To clarify this point, let us estimate the distance s from the horizon radius r_0 upto which this radiation density is appreciable. Suppose the temperature of the ECO as seen at infinity

is T_{ECO} . The radiated quanta suffer a redshift as they move out of the gravitational potential of the ECO. Thus the effective temperature of the radiation at a radius r , measured in a local orthonormal frame with time direction along t , is

$$T_{\text{ECO}}(r) = q(r)T_{\text{ECO}}, \quad (2.17)$$

where $q(r)$ is the redshift parameter (2.13). Using (2.14) for the value of $q(r)$ in the Rindler region $(r - r_0)/r_0 \ll 1$, for the black hole metric (2.6), we find that the temperature at a distance s from the horizon radius r_0 is

$$T_{\text{ECO}}(s) \approx \frac{2r_0}{(d-2)s} T_{\text{ECO}}. \quad (2.18)$$

Assuming that T_{ECO} is of the same order as the Hawking temperature $T_H \sim r_0^{-1}$, we have

$$T_{\text{ECO}}(s) \sim \frac{1}{s}. \quad (2.19)$$

Thus we see that at small s , the local temperature is very high, and in fact this temperature reaches planck scale at planck distance $s \sim l_p$ from the horizon radius. The energy density of a massless quantum field at temperature T is

$$\rho = aT^{d+1}, \quad (2.20)$$

where a is a constant of order unity, depending on the dimension d and the spin of the quantum field. For a scalar field in 3+1 dimensions

$$a = \frac{\pi^2}{30}. \quad (2.21)$$

If there is nonzero stress energy outside R_{ECO} , then how should we capture the compactness of the ECO through the condition (2.11) on R_{ECO} ? In particular, there is a singular situation that formally satisfies the conditions ECO1, ECO2, but which we should exclude from our consideration of ECOs. As we will discuss later in section 6, the Einstein equations allow a ‘truncated isothermal star’, which has the following structure. There is an isothermal photon gas filling the region $0 < r < R$, with the matter density truncated in some way at $r = R$. The density rises to infinity at $r \rightarrow 0$, and the redshift $q(r)$ also diverges at $r \rightarrow 0$. Thus one could place a surface just outside $r = 0$ and find a high redshift at this surface, satisfying condition ECO2. The surface also has a very small radius, so it would formally satisfy the spirit of the requirement ECO1. But such an object is not what we would consider an ECO for our purposes, since almost all its mass is outside the high redshift surface that we have defined. Thus we would like to impose a condition on our ECO which says that there is very little matter outside the compactness scale s_c

Note that the energy density of thermal radiation will typically fall off as a power law as we go out from the ECO. Thus we cannot ask that it be exactly zero at some given distance from the ECO surface, but we can ask that its effects not be relevant if we are sufficiently far from the ECO surface. We do this by requiring that outside the compactness scale s_c , the geometry is close to the metric of the black hole:

ECO3: At distances $s > \left(\frac{M}{m_p}\right)^{\frac{2}{(d-2)(d+1)}} l_p$ from the black hole horizon radius r_0 , the geometry is well approximated by the black hole metric (2.6).

In particular, at distances $s > s_c$ from the black hole radius r_0 , the redshift factor is of order the redshift for the black hole metric

$$q_{\text{ECO}}(r) \sim \left(1 - \frac{r_0^{d-2}}{r^{d-2}}\right)^{-\frac{1}{2}}. \quad (2.22)$$

In section 6.3 we will check that it is consistent to impose condition ECO3; i.e., we will verify that the stress-tensor of the thermal radiation near the ECO surface does not significantly distort the black hole metric at distances $s \gtrsim s_c$ from the horizon radius r_0 .

2.4 A relation following from condition ECO1

The condition ECO1 says that semiclassical dynamics is a good approximation at $r > R_{\text{ECO}}$. From the discussion of section 2.3, we see that there will in general be a nonvanishing energy density $T^t_t = -\rho$ in this region. We can then use the ansatz (2.6) for the metric, and solve the equation $G_{tt} = 8\pi G T_{tt}$ with this energy density. In 3+1 dimensions we get

$$e^{-2\beta(r)} = 1 - \frac{2GM(r)}{r}. \quad (2.23)$$

For a star, we have

$$M(r) = \int_0^r dr 4\pi r^2 \rho(r). \quad (2.24)$$

For an ECO, the region $0 < r < R_{\text{ECO}}$ can have large quantum gravitational effects, and thus may not be well approximated as a smooth manifold. Thus we do not wish to integrate over r in this region. But we can compute $M(r)$ by integrating the mass density *outside* the ECO, using the fact that the mass as seen from infinity is M :

$$M(r) = M - \int_r^\infty dr 4\pi r^2 \rho(r). \quad (2.25)$$

In $d+1$ dimensions, we have

$$e^{-2\beta(r)} = 1 - \frac{\mu GM(r)}{r^{d-2}}, \quad \mu = \frac{16\pi}{(d-1)\Omega_{d-1}}, \quad (2.26)$$

with

$$M(r) = M - \int_r^\infty dr \Omega_{d-1} r^{d-1} \rho(r). \quad (2.27)$$

The regularity of the ECO solution thus yields the following requirement. In the region $r > R_{\text{ECO}}$ we must have everywhere

$$1 - \frac{\mu GM(r)}{r^{d-2}} > 0. \quad (2.28)$$

3 The vacuum stress-energy near an ECO

In section 2.3 we talked about the energy density of radiation outside the ECO. But even if our object has a temperature $T = 0$, there is still an important energy to consider outside the surface of the object. There is a nonvanishing vacuum stress-energy of quantum fields in the region around the object, caused by the behavior of field modes in the metric created by the object. As we will note below, for temperatures which are of order the Hawking temperature, this vacuum stress-energy is of the same order as the stress-energy of the radiation near the surface. Thus this vacuum energy will play an important role in our analysis.

We will begin by recalling the computation of vacuum energy for the Schwarzschild hole. We will then note that an ECO has, to leading order, the *same* vacuum energy as a black hole. Taking into account the thermal radiation just outside the ECO, we will obtain the total stress energy in this near-surface region.

3.1 The vacuum stress-tensor near a black hole horizon

The vacuum energy in a spacetime depends in general on the choice of the quantum state for the fields. In a black hole spacetime, some commonly considered states are the Unruh vacuum, the Hartle-Hawking vacuum and the Boulware vacuum. In 3+1 dimensions the vacuum energy for these states was computed in [33], using methods developed in [34–39]. This computation is in general quite complicated, but there is a simple way to get the answer for the quantity we need: the vacuum stress energy for the Boulware vacuum to leading order close to the horizon.

Let us first recall how the computation of the vacuum stress-energy proceeds in general for the black hole metric (2.6). Consider for simplicity a scalar field $\hat{\phi}$ satisfying $\square\hat{\phi} = 0$. We expand $\hat{\phi}$ in modes in the region $r > r_0$

$$\hat{\phi} = \sum_{\{l\},k} \left(\hat{a}_{\{l\},k} f_{\{l\},k}(r) Y_{\{l\}}(\{\Phi\}) e^{-i\omega_{\{l\},k} t} + \hat{a}_{\{l\},k}^\dagger f_{\{l\},k}^*(r) Y_{\{l\}}^*(\{\Phi\}) e^{i\omega_{\{l\},k} t} \right), \quad (3.1)$$

where $\{l\}$ denote the quantum numbers of the angular harmonic and $\{\Phi\}$ denote the angular variables on Ω_{d-1} . The effective potential felt by these modes $f_{\{l\},k}(r)$ is sketched in fig.2(a). The potential vanishes near the horizon, and also at infinity, with a barrier in the region in between.

Using the above modes, one computes the correlator

$$\langle \Psi | \hat{\phi}(x) \hat{\phi}(y) | \Psi \rangle, \quad (3.2)$$

for infinitesimally separated x, y . The computation of this correlator requires knowledge of the quantum state $|\Psi\rangle$ of the field $\hat{\phi}$. We then find the expectation value of the stress-energy tensor by computing taking appropriate derivatives in x, y , subtracting a normal ordering constant, and then taking the limit $x \rightarrow y$.

Knowledge of the above procedure will be useful to us below, but for now we note that for the leading order stress-tensor in the Boulware vacuum, there is an easier way to obtain the result. The argument proceeds as follows. In the Hartle-Hawking vacuum, the black hole is in equilibrium with its radiation. The geometry is smooth at the horizon, and there is no flux into or out of the horizon. Thus to leading order the stress-energy tensor is zero around the horizon. (Here by ‘leading order’ we mean that we are ignoring contributions of order $\langle T^\mu_\nu \rangle \sim r_0^{-(d+1)}$

which arise from the energy density of quanta with wavelength $\lambda \sim r_0$, and terms arising from the anomaly; these terms are regular at the horizon.) We can understand this vanishing of the stress energy by going to Rindler coordinates (2.8) near the horizon. Then the Hartle-Hawking vacuum is like the Minkowski vacuum, which has a vanishing stress tensor.

Now consider the Boulware vacuum $|0\rangle_B$. This vacuum state is obtained by requiring

$$\hat{a}_{\{l\},k}|0\rangle_B = 0, \quad (3.3)$$

for the operator modes in (3.1). To understand the nature of this state, consider the near horizon Rindler region. In this region the modes $f_{\{l\},k}(r)$ in (3.1) are Rindler modes and the Boulware vacuum is the Rindler vacuum. In Rindler coordinates, the Minkowski vacuum appears to be populated with Rindler excitations at a temperature

$$T(s) = \frac{1}{2\pi s}. \quad (3.4)$$

Since the Minkowski vacuum has vanishing stress tensor, the stress tensor of the Rindler vacuum is given by the *negative* of the stress tensor of thermal radiation at temperature (3.4).

The Hawking temperature of the black hole in $d+1$ dimensions is

$$T_H = \frac{(d-2)}{4\pi r_0}, \quad (3.5)$$

and (3.4) is just this temperature times the redshift factor at distance s from the horizon. In terms of the coordinate r , the local temperature $T_H(r)$ is

$$T_H(r) = q(r) T_H = \left(1 - \frac{r_0^{d-2}}{r^{d-2}}\right)^{-\frac{1}{2}} \frac{(d-2)}{4\pi r_0} \approx \frac{(d-2)^{\frac{1}{2}}}{4\pi r_0^{\frac{1}{2}}(r-r_0)^{\frac{1}{2}}}, \quad (3.6)$$

where the final expression is the approximation appropriate for the Rindler region $r-r_0 \ll r_0$. The stress tensor of the Boulware vacuum is then

$$T^\mu_\nu = \text{diag}\{-\rho(r), p(r), \dots, p(r)\}, \quad (3.7)$$

with

$$\rho(r) = -aT_H(r)^{d+1}, \quad (3.8)$$

and

$$p(r) = \frac{1}{d}\rho(r). \quad (3.9)$$

3.2 The stress tensor near an ECO

Now we will argue that if we have an ECO at temperature $T_{\text{ECO}} = 0$, then the stress tensor in the region just outside R_{ECO} has the *same* value, to a first approximation, as the stress tensor (3.7)-(3.9) in the Boulware vacuum of the black hole. The key point will be that due to the compactness of the ECO, the analogues of the wavemodes $f_{\{l\},k}(r)$ in the ECO will have a large number of oscillations in the region $r > R_{\text{ECO}}$. These oscillations allow us to make local wavepackets out of these modes, and the local value of the stress tensor can be obtained to a

good approximation from such wavepackets. Thus the detailed nature of the wavemode in the interior region $r < R_{\text{ECO}}$ becomes irrelevant to the computation of the stress-energy outside R_{ECO} .

First consider the wavemodes $f_{\{l\},k}(r)$ in the black hole metric. These modes have the form

$$f_{\{l\},k}(r) = \frac{\chi_{\{l\},k}(r)}{r^{\frac{d-1}{2}}}, \quad (3.10)$$

with $\chi_{\{l\},k}(r)$ satisfying the equation

$$-\frac{d^2}{dr^{*2}}\chi_{\{l\},k} + \left(1 - \frac{r_0^{d-2}}{r^{d-2}}\right) \left(\frac{(d-1)^2}{4} \frac{r_0^{d-2}}{r^d} + \frac{L^2 + \frac{1}{4}(d-1)(d-3)}{r^2}\right) \chi_{\{l\},k} = \omega^2 \chi_{\{l\},k}, \quad (3.11)$$

where $\omega = |k|$ and $L^2 = l(l+d-2)$, $l = 0, 1, 2, \dots$ is the value of the quadratic Casimir describing angular momentum. We have defined the ‘tortoise’ coordinate r^* through $dr^* = \left(1 - \frac{r_0^{d-2}}{r^{d-2}}\right)^{-1} dr$, which in the near horizon region gives

$$r^* \approx \frac{r_0}{(d-2)} \ln\left(\frac{r - r_0}{r_0}\right) \approx -\frac{2r_0}{(d-2)} \log \frac{r_0}{s}. \quad (3.12)$$

For later use we define the ‘effective potential’ appearing in (3.11)

$$V_{\text{eff}} \equiv \left(1 - \frac{r_0^{d-2}}{r^{d-2}}\right) \left(\frac{(d-1)^2}{4} \frac{r_0^{d-2}}{r^d} + \frac{L^2 + \frac{1}{4}(d-1)(d-3)}{r^2}\right). \quad (3.13)$$

In the near horizon region, $V_{\text{eff}} \rightarrow 0$, and we have

$$-\frac{d^2}{dr^{*2}}\chi_{\{l\},k} = \omega^2 \chi_{\{l\},k}, \quad (3.14)$$

which gives

$$\chi \sim e^{\pm i\omega r^*}. \quad (3.15)$$

Suppose we look at the region $r_0 + \epsilon < r \lesssim 2r_0$, for $\epsilon \ll r_0$. The corresponding range for r^* is

$$\frac{r_0}{(d-2)} \ln\left(\frac{\epsilon}{r_0}\right) < r^* < 0. \quad (3.16)$$

The phase of χ is seen to oscillate a number of times n given by

$$n \approx \frac{\omega}{2\pi} \frac{r_0}{(d-2)} \ln\left(\frac{r_0}{\epsilon}\right) \approx \frac{\omega}{2\pi} \frac{2r_0}{(d-2)} \ln\left(\frac{2}{(d-2)^{\frac{1}{2}}} \frac{r_0}{s}\right), \quad (3.17)$$

where in the last step we have written the coordinate interval ϵ in terms of the proper s distance from the horizon. Note that $\omega r_0 \sim 1$, since the energy of the typical quantum emitted is of order the black hole temperature $\sim 1/r_0$. For ϵ/r_0 small (equivalently, s/r_0 small), we find that the number of oscillations near the horizon is $n \gg 1$. As we approach the horizon, we have $\epsilon \rightarrow 0$ and the number of oscillations becomes infinite. We depict these oscillations in fig. 1(a).

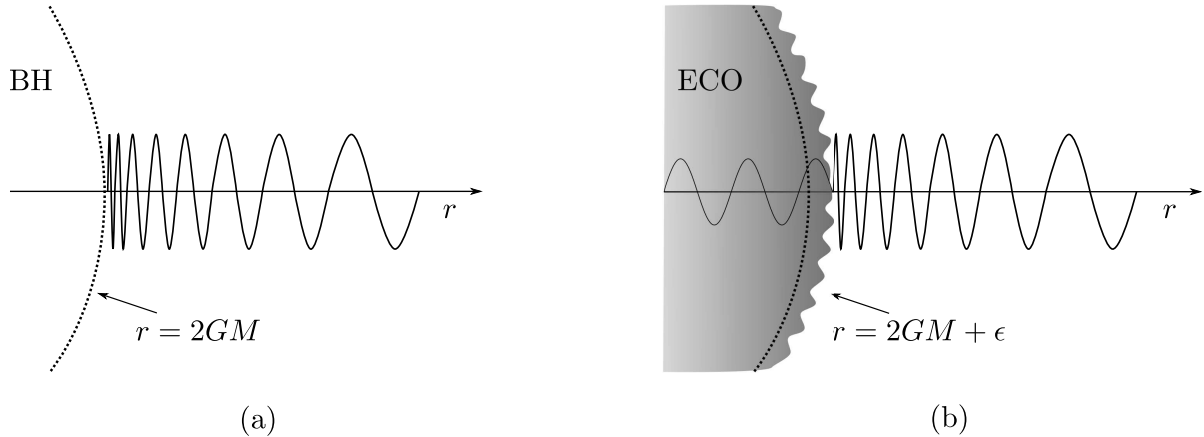


Figure 1: (a) In the black hole geometry, a wavemode oscillates an infinite number of times as it approaches the horizon. (b) In the ECO geometry, the wavemode oscillates a large number of times $n \gg 1$ before entering the ECO surface at R_{ECO} .

Now consider the computation of the stress tensor for an ECO. We should first expand the field $\hat{\phi}$ in terms of field modes that satisfy $\square \hat{\phi} = 0$ in the metric produced by the ECO:

$$\hat{\phi} = \sum_{\{l\},k} \left(\hat{b}_{\{l\},k} g_{\{l\},k}(r) Y_{\{l\}}(\{\Phi\}) e^{-i\omega_{\{l\},k} t} + \hat{b}_{\{l\},k}^\dagger g_{\{l\},k}^*(r) Y_{\{l\}}^*(\{\Phi\}) e^{i\omega_{\{l\},k} t} \right). \quad (3.18)$$

Consider the situation where the ECO is at temperature $T_{\text{ECO}} = 0$. Then the quantum field $\hat{\phi}$ will be in its lowest energy state $|\Psi_{\text{ECO},0}\rangle$ in the background geometry created by the ECO. This state is described by

$$\hat{b}_{\{l\},k} |\Psi_{\text{ECO},0}\rangle = 0. \quad (3.19)$$

A priori, the modes $g_{\{l\},k}(r)$ will depend on the metric in the outside region $r > R_{\text{ECO}}$ as well as the metric in the inside region $r < R_{\text{ECO}}$; in fact they are required to satisfy a smoothness condition at $r = 0$ which is in the region $r < R_{\text{ECO}}$. But due to the compactness of the ECO, the modes $g_{\{l\},k}(r)$ will have a large number of oscillations n in the region $R_{\text{ECO}} < r < 2r_0$. Note that by condition ECO1, we have $s_{\text{ECO}} \ll s_c$, where s_c is the compactness length scale s_c defined in (2.12). From (3.17) we find, using $r_0^{d-2} = \mu GM$,

$$n \gg \frac{\omega}{2\pi} \frac{2r_0}{(d-2)} \ln \left(\frac{2}{(d-2)^{\frac{1}{2}}} \frac{r_0}{s_c} \right) \sim \omega r_0 \ln \left(\frac{M}{m_p} \right) \sim \ln \left(\frac{M}{m_p} \right), \quad (3.20)$$

where in the last step we have again set $\omega r_0 \sim 1$ since we have in mind a temperature for the ECO which is of order the black hole temperature. This large number of oscillations is depicted in fig.1(b). Due to this large number of oscillations of $g_{\{l\},k}(r)$ in the region just outside R_{ECO} , any computation using these modes can be captured equally well by local wavepackets built from these modes. Thus we can compute the quantity $\langle \Psi_{\text{ECO},0} | \hat{\phi}(x) \hat{\phi}(y) | \Psi_{\text{ECO},0} \rangle$, to a good approximation, by using the form of the modes $g_{\{l\},k}(r)$ in the region $r > R_{\text{ECO}}$. If we assume that this region is just given by the Schwarzschild geometry (2.6) with mass M , then the wavepackets made from modes $g_{\{l\},k}(r)$ in the region $r > R_{\text{ECO}}$ will be approximately the same

as wavepackets made from modes $f_{\{l\},k}(r)$ in the black hole geometry. In this approximation, we will get the same value for the stress tensor in the ECO as we had in the black hole. Thus we will have in the region $r > R_{\text{ECO}}$

$$T^\mu{}_\nu = \text{diag}\{-\rho(r), p(r), \dots, p(r)\}, \quad (3.21)$$

with

$$\rho(r) = -a T_{\text{H}}(r)^{d+1}, \quad p = \frac{1}{d} \rho(r). \quad (3.22)$$

3.3 The ECO at a general temperature T

We have seen above that the ECO at temperature $T_{\text{ECO}} = 0$ has a negative energy density near its surface just like the negative energy density of the Boulware vacuum. This result was based on the assumption that the metric in the region of interest was well approximated by the Schwarzschild metric. Let us continue with this approximation in mind and discuss the case of an ECO at a temperature $T_{\text{ECO}} \neq 0$. Later we will discuss how to take into account the departure of the metric at $r > R_{\text{ECO}}$ from the Schwarzschild form.

Thus suppose the ECO has a temperature at infinity given by T_{ECO} . At a radius r , the redshift results in a local temperature

$$T_{\text{ECO}}(r) = q(r) T_{\text{ECO}}, \quad (3.23)$$

where $q(r)$ is given by (2.14). This radiation generates a stress tensor of the form (3.21) with

$$\rho(r) = a T_{\text{ECO}}(r)^{d+1}, \quad p = \frac{1}{d} \rho(r). \quad (3.24)$$

Taking into account the vacuum stress-energy (3.21), (3.22) we find that, with the above mentioned approximations, the total stress tensor in the region just outside the ECO is of the form (3.21) with

$$\rho(r) = a \left(T_{\text{ECO}}^{d+1} - T_{\text{H}}^{d+1} \right) q(r)^{d+1}, \quad p = \frac{1}{d} \rho(r). \quad (3.25)$$

4 Relating S to T

Suppose that we were *given* that the temperature $T_{\text{ECO}}[M]$ of an ECO had to be the same as the temperature of a black hole $T_{\text{H}}[M]$. Then, as we argue in this section, two conclusions follow. First, the entropy $S_{\text{ECO}}[M]$ of the ECO will have to agree with the black hole entropy $S_{\text{bek}}[M]$. Second, the radiation rate from the ECO $\Gamma_{\text{ECO}}[M]$ will have to agree with the radiation rate $\Gamma_{\text{H}}[M]$ from the black hole.

Having made these arguments, we will be left with the task of showing that $T_{\text{ECO}}[M] = T_{\text{H}}[M]$, which will be the main task of this paper. This task will be tackled in the remaining sections.

4.1 Relating the entropy S_{ECO} to the temperature

Consider the entropy of any isolated body which has a large number of degrees of freedom. We have the relation

$$TdS = dE. \quad (4.1)$$

Now suppose we are given that our ECO has an temperature $T_{\text{ECO}}[M]$ that matched the Hawking temperature of the black hole, then we would have

$$S_{\text{ECO}} = \int T_{\text{ECO}}^{-1} dM = \int \left(\frac{4\pi r_0}{d-2} \right) \left(\frac{(d-2)r_0^{d-3}}{G\mu} \right) dr_0 = \frac{\Omega_{d-1} r_0^{d-1}}{4G} = \frac{A}{4G}, \quad (4.2)$$

where we have used (3.5) and (2.7). The RHS of (4.2) is the Bekenstein Hawking entropy for the $d+1$ dimensional hole.

The above computation is not new; it is just the standard one through which the Bekenstein entropy of a black hole was obtained after the discovery that the hole radiates at temperature T_H [1, 2]. This value of the black hole entropy was then reproduced through the Gibbons-Hawking computation of a Euclidean path integral [40]. Here we are just noting that *any* isolated object with the same temperature function $T_H[M]$ as the black hole will have the same entropy as the black hole. The fact that the object is isolated tells us that we do not have to consider additional terms in (4.1) like PdV or $\mu_i dN_i$ (here μ_i are chemical potentials and N_i are the corresponding particle numbers).

4.2 Relating the emission rate Γ_{ECO} to the temperature

We now address the radiation rate from the ECO. First consider a normal body, like a ball of steel. The rate of radiation from the ball cannot be determined if we just know the temperature T . For example, a ball painted black will radiate more energy than a ball painted white; this is because emission and absorption are related by detailed balance, and a black ball absorbs more readily than a white ball. Further, if the wavelength λ of the emitted radiation is order $\lambda \gtrsim R$ where R is the size of the body, then the radiation rate can also depend on the details of the shape of the body, and not just on its surface area.

Now consider our ECO. Since the radius of the ECO is very close to the radius of the corresponding black hole, the surface area of the ECO will be almost the same as the surface area of the hole. But we have not assumed anything else about the nature of the surface of the ECO. Further, the wavelength λ of the radiation from a hole is $\lambda \sim r_0$, where r_0 is the radius of the hole. It may therefore appear that even if we are given that the ECO is at the same temperature T_H as the corresponding black hole, we may not be able to say anything about the rate of radiation from the ECO.

But as we will now note, such is not the case. The radiation rate Γ_{ECO} from the ECO must equal the radiation rate Γ_H to leading order. We will first review the derivation of Hawking radiation from a black hole using Schwarzschild coordinates. Here we will note that the near horizon region is filled with a hot gas of quanta at the local Rindler temperature. These quanta tunnel through a high barrier at larger r and reach infinity to give Hawking radiation. Next we will consider an ECO at the same temperature. The near surface region will be filled with quanta at the same temperature as the corresponding black hole, and the barrier through which they must tunnel will also be approximately the same. Thus the radiation profile will agree

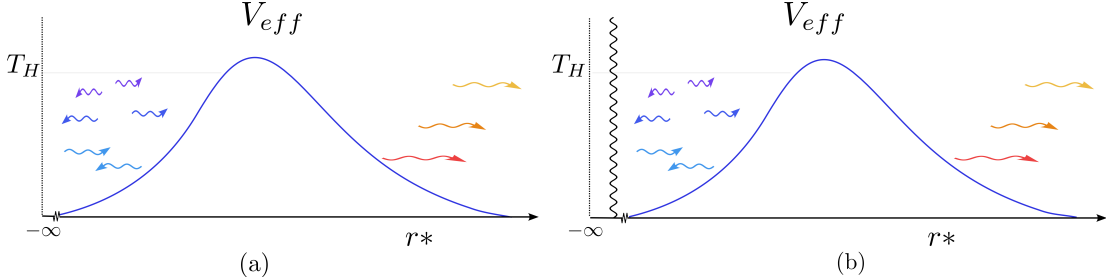


Figure 2: (a) In the black hole geometry, Rindler quanta are trapped near the horizon by the potential V_{eff} . Some low l quanta manage to tunnel through this potential and escape to infinity as Hawking radiation. (b) In The ECO, we have a similar set of thermal quanta trapped near the ECO surface; these quanta must tunnel through essentially the same potential to escape as radiation.

between the black hole and the ECO. A crucial point in this argument will be the compact nature of the ECO; this compactness leads to a separation between the near surface region which contains the hot gas of quanta, and the region further out which contains the potential barrier.

For radiation from the black hole, we consider the wave-equation (3.11) for modes in the black hole geometry. We look at three regions: (i) close to the horizon (ii) further out, in the region of the potential barrier (iii) the region near infinity. The setup is pictured in fig. 2(a).

(i) Close to the horizon, the effective potential V_{eff} vanishes due to the factor $1 - \frac{r_0^{d-2}}{r^{d-2}}$, and the wave-equation becomes

$$-\frac{d^2}{dr^{*2}}\chi_{\{l\},k} = \omega^2\chi_{\{l\},k}. \quad (4.3)$$

In this near-horizon region we can describe the geometry by the Rindler coordinates (2.8), and (4.3) yields the Rindler modes for our field $\hat{\phi}$. In this spacetime region it is useful to think in terms of the proper distance s from the horizon radius r_0 . The spacetime is filled with a thermal gas of Rindler excitations at temperature $T_H(s) = \frac{1}{2\pi s}$; this temperature is just the appropriately blueshifted value of the Hawking temperature T_H at infinity. The radiated quanta have energy of order the Hawking temperature; thus we have $\omega \sim T_H \sim 1/r_0$ in (4.3).

(ii) At larger r , the potential V_{eff} becomes important, and gives a high barrier for the modes $\chi_{\{l\},k}$. The reason that the barrier is high is that the angular momentum L is large for a typical mode in the thermal gas near $r = r_0$. At a proper distance s from the horizon radius r_0 , the wavelength of the typical quantum is $\lambda \sim s$, and thus the typical value of L in the thermal gas is

$$L \sim \frac{r_0}{s}. \quad (4.4)$$

The barrier height for $s \ll r_0$ is (transforming coordinates from r to s)

$$V_{eff} \approx \frac{s^2 L^2}{r_0^4}. \quad (4.5)$$

Thus at distances $s \sim r_0/L$, the potential term in (3.11) becomes of order $1/r_0^2 \sim \omega^2$. At larger s , the potential rises to a value higher than the energy term ω^2 on the RHS of (3.11), and at $s \sim r_0$, we get

$$V_{eff} \sim \frac{L^2}{r_0^2} \sim L^2 \omega^2. \quad (4.6)$$

We see that for $L \gg 1$, the height of the barrier is much larger than the energy term ω^2 in the wave-equation (3.11).

- (iii) At $r \rightarrow \infty$, we again have $V_{eff} \rightarrow 0$, and we get freely propagating waves satisfying (4.3). From the discussion in (ii) above, the potential V_{eff} confines the the large L angular harmonics to a small distance $s \sim r_0/L$ from the horizon, and only models with $L \sim 1$ tunnel through the barrier and escape to infinity.

Thus we can derive the rate of Hawking radiation from a black hole as follows. Consider any spherical harmonic $Y_{\{l\}}(\{\Phi\})$. The corresponding radial function $\chi_{\{l\},k}$ gives a freely traveling outward wave at $r^* \rightarrow -\infty$. This wave encounters the potential barrier V_{eff} , whereupon a part of the wave gets reflected back and a part tunnels out and escapes to infinity as ‘Hawking radiation’. The large L modes get reflected back strongly; thus only modes with $L \sim 1$ escape to infinity. Using the potential V_{eff} we can compute the probability $P[\{l\}, \omega]$ for the wavemode to tunnel from the region $r^* \rightarrow -\infty$ out to $r^* \rightarrow \infty$.

We assume an occupation number of the modes $\chi_{\{l\},k}$ at $r^* \rightarrow -\infty$ given by the local Rindler temperature $T_H(s) = 1/(2\pi s)$. This occupation number determines the flux of such modes that is incident on the potential barrier from the side $r^* \rightarrow -\infty$. Multiplying this flux by the probability of tunneling $P[\{l\}, \omega]$ gives the radiation rate $\Gamma_H[\{l\}, \omega]$.

Note that in this derivation of the Hawking radiation rate $\Gamma_H[\{l\}, \omega]$ we have used only the exterior of the hole $r > r_0$. Hawking’s original derivation had considered modes that straddle the horizon; these modes get distorted to produce a pair of quanta, one inside the hole and one escaping to infinity as radiation. In the derivation above, the smooth horizon that Hawking assumed is taken into account by the assumption of the thermal Rindler state just outside the horizon; this thermal state is equivalent to the local Minkowski vacuum at the horizon in Kruskal coordinates.

Now consider the radiation from the ECO. We depict the situation in fig. 2(b). In the black hole geometry (2.6), the coordinate r^* goes to $-\infty$ as $r \rightarrow r_0^+$ (eq. (3.12)). In the ECO, the Schwarzschild geometry gets completely modified at $r < R_{ECO}$, but note that $R_{ECO} - r_0$ is small. By condition ECO3, the Schwarzschild geometry is obtained to a good approximation for points outside the compactness scale s_c . From (3.12), this region is

$$r^* \gtrsim -r_0 \ln \frac{r_0}{s_c}. \quad (4.7)$$

In the region

$$-r_0 \ln \frac{r_0}{s_c} \lesssim r^* \ll r_0, \quad (4.8)$$

the effective potential V_{eff} is small due to the vanishing of the factor $(1 - \frac{r_0^{d-2}}{r^{d-2}})$, and we get the free-field behavior (3.14),(3.15) for $\chi_{\{l\},k}$ in (3.11). We have a gas of quanta in this region

at a local temperature

$$T_{\text{ECO}}(s) = q(s) T_{\text{ECO}} \approx \frac{T_{\text{ECO}}}{T_{\text{H}}} \frac{1}{2\pi s}, \quad (4.9)$$

where $q(s)$ is given by (2.14). The potential V_{eff} in the region $r^* \gtrsim -r_0 \ln \frac{r_0}{s_c}$ is, by condition ECO3, approximately the same as in the case of the black hole, so the tunneling probability for a quantum with a given L, ω will be the same, to leading order, for the black hole and the ECO.

Thus we can compute the radiation from the ECO in a manner that parallels the computation of radiation from the black hole. In the ECO geometry, we have a thermal distribution of quanta near $r = R_{\text{ECO}}$ with the temperature (4.9). Quanta with large L reflect off the barrier and return to the surface of the ECO, where they thermalize with the degrees of freedom in the ECO and get reemitted to the region $r > R_{\text{ECO}}$ (with in general a different value of L). The quanta with low L which escape to infinity determine the radiation rate $\Gamma_{\text{ECO}}[\{l\}, \omega]$.

The probability of tunneling for these low L quanta is the same, to leading order, as the probability of tunneling in the black hole geometry, since for low L the potential barrier is significant only in region $r - r_0 \sim r_0$, which is far from the ECO surface at $r = R_{\text{ECO}}$.

If $T_{\text{ECO}} = T_{\text{H}}$, then the flux incident on the barrier from $r^* \rightarrow -\infty$ is the same, to leading order, for the ECO and the black hole. Thus we will get

$$\Gamma_{\text{ECO}}[\{l\}, \omega] \approx \Gamma_{\text{H}}[\{l\}, \omega]. \quad (4.10)$$

Let us recall how the conditions ECO1-ECO3 were important in obtaining the above conclusion. First consider the condition ECO1. As we have seen, only modes with $L \sim 1$ are radiated in an appreciable manner. The effective potential $V_{\text{eff}}(r)$ for such modes is peaked around $(r - r_0)/r_0 \sim 1$, and vanishes for $(r - r_0)/r_0 \ll 1$ due to the factor $1 - \frac{r_0^{d-2}}{r^{d-2}}$. If $(R_{\text{ECO}} - r_0)/r_0$ is not very small, then the radiated modes in the ECO pass through only that part of the potential which is in the region $r > R_{\text{ECO}}$ in contrast to modes in the black hole which tunnel through the full range $r_0 < r < \infty$. For $(R_{\text{ECO}} - r_0)/r_0 \ll 1$, the modes with $L \sim 1$ encounter essentially the same potential in the ECO and in the black hole.

The condition ECO2 of high redshift at the surface of the ECO is important because it implies a high local temperature for quanta near $r = R_{\text{ECO}}$. This high temperature translates to a short wavelength, which gives a well defined local thermal distribution of quanta in the region $(r - R_{\text{ECO}})/r_0 \ll 1$. Having such a thermal distribution allows us to separate the radiation computation into two parts. One part is the computation of a tunneling probability through the barrier (which peaks at $r - r_0 \sim r_0$) and the other part is the computation of the number density of quanta present near $r = R_{\text{ECO}}$. If we did not have such a separation, then we would not be able to assume a black body distribution of quanta at some local temperature $T_{\text{ECO}}(r)$; the potential V_{eff} would become relevant even for finding the distribution of modes near $r = R_{\text{ECO}}$.

Finally, the condition ECO3 allowed us to use the effective potential V_{eff} in the region from $s \sim s_c$ out to infinity.

5 A heuristic argument for the relation $T_{\text{ECO}} \approx T_{\text{H}}$

In section 4 we have seen that *if* we are given that $T_{\text{ECO}} = T_{\text{H}}$, then the entropy and radiation rates of the ECO will agree with the corresponding quantities for the black hole. We now pass on to our main task: arguing that an ECO that satisfies our conditions ECO1-ECO3 cannot have an arbitrary temperature, but rather must have $T_{\text{ECO}} \approx T_{\text{H}}$. It will be clear from our discussion that the approximation in this relation will become better as we take the distance s_{ECO} to be smaller.

In this section, we will make our first pass at arguing for this equality of temperatures, in the process obtaining the compactness condition (2.11). In this first pass, we will not be completely consistent in our approximations, in the following sense. We will need to use the energy density of the radiation near the surface of the ECO. This energy density at a radius r depends on the value of the redshift at r . This redshift, in turn, is affected by the energy density of the radiation itself. But in the analysis of this section, we will ignore this feedback of the radiation on the metric, assuming instead the redshift implied by the usual black hole metric in the region $r > R_{\text{ECO}}$. In the next section, we will remedy this inaccuracy by solving the Tolman-Oppenheimer-Volkoff equation in the region near $r = R_{\text{ECO}}$.

5.1 The energy of radiation near the ECO

Consider the near-surface region outside R_{ECO} , described by the condition $r - R_{\text{ECO}} \ll r_0$. As we saw in section 4, the effective potential V_{eff} traps the radiation from the ECO in this near-surface region, so that we have a thermal gas of quanta at some local temperature $T_{\text{ECO}}(r)$ which depends on r . Far from the ECO we just have outgoing radiation in low l harmonics, so the energy density is very low. Thus we will take the thermal distribution of the near-surface region to be truncated so that it is nonvanishing only in the the region $r \lesssim 2r_0$; in fact as we will see the energy density is appreciable only very close to $r = R_{\text{ECO}}$.

This radiation in the region $R_{\text{ECO}} < r < 2r_0$ has a total energy which we will call E_{rad} . Note that due to the negative vacuum energy in the region outside the ECO, E_{rad} will be positive if $T_{\text{ECO}} > T_{\text{H}}$ and E_{rad} will be negative if $T_{\text{ECO}} < T_{\text{H}}$.

Now consider the mass function $M(r)$ defined in (2.27). Since the mass at infinity is M , we will have

$$M(R_{\text{ECO}}) = M - E_{\text{rad}}. \quad (5.1)$$

The quantity $M(R_{\text{ECO}})$ can be thought of as the mass contained inside the ‘core’ of the ECO – the region which contains any nontrivial quantum gravitational dynamics. Recall that the horizon radius r_0 of a black hole is related to its mass M by the relation (2.7). Correspondingly, we define a radius \tilde{r}_0 through

$$\tilde{r}_0^{d-2} = \mu GM(R_{\text{ECO}}), \quad (5.2)$$

where the radius \tilde{r}_0 would be the radius of a black hole with mass $M(R_{\text{ECO}})$ if we had a Schwarzschild geometry with mass $M(R_{\text{ECO}})$. The equation (2.28) requires

$$1 - \frac{\mu GM(R_{\text{ECO}})}{R_{\text{ECO}}^{d-2}} > 0, \quad (5.3)$$

so that

$$\tilde{r}_0 < R_{\text{ECO}}. \quad (5.4)$$

Thus \tilde{r}_0 is a radius that is inside a region that we will not directly address. Nevertheless, the coordinate separation $R_{\text{ECO}} - \tilde{r}_0$ will play an important role in the discussion below. We will generally find that $\tilde{r}_0 - r_0 \ll r_0$ and so in many steps below we will use the approximation

$$\tilde{r}_0 \approx r_0, \quad (5.5)$$

to simplify our expressions.

Consider the geometry generated by a mass $M(R_{\text{ECO}})$ confined within the radius $r = R_{\text{ECO}}$, and no energy density at $r > R_{\text{ECO}}$. For $r > R_{\text{ECO}}$ the metric for this geometry is of the Schwarzschild form

$$ds^2 = -\left(1 - \left(\frac{\tilde{r}_0}{r}\right)^{d-2}\right)dt^2 + \frac{dr^2}{1 - \left(\frac{\tilde{r}_0}{r}\right)^{d-2}} + r^2 d\Omega_{d-1}^2. \quad (5.6)$$

As noted above, in the actual ECO, there is a nonzero energy density ρ in the region $r > R_{\text{ECO}}$. But we will be ignoring the deformation of the metric due to this ρ in some of steps below; in these steps we will refer to the metric (5.6).

With the metric (5.6), the redshift at a radius r is given by

$$\tilde{q}(r) = (-g_{tt}(r))^{-\frac{1}{2}} \approx \frac{\tilde{r}_0^{\frac{1}{2}}}{(d-2)^{\frac{1}{2}}(r - \tilde{r}_0)^{\frac{1}{2}}} \approx \frac{r_0^{\frac{1}{2}}}{(d-2)^{\frac{1}{2}}(r - \tilde{r}_0)^{\frac{1}{2}}}. \quad (5.7)$$

Here we have added a tilde to the variable q to denote the fact that this redshift \tilde{q} corresponds to the redshift in the geometry with horizon radius \tilde{r}_0 . The energy density at radius r is then

$$\rho(r) = a \left(T_{\text{ECO}}^{d+1} - T_{\text{H}}^{d+1} \right) \tilde{q}(r)^{d+1}. \quad (5.8)$$

The total energy of this radiation in the region $R_{\text{ECO}} < r < \infty$ is

$$\begin{aligned} E_{\text{rad}} &\approx \int_{r=R_{\text{ECO}}}^{\Lambda} dr \Omega_{d-1} r^{d-1} \rho(r), \\ &\approx a \left(T_{\text{ECO}}^{d+1} - T_{\text{H}}^{d+1} \right) \Omega_{d-1} \int_{r=R_{\text{ECO}}}^{\Lambda} dr r^{d-1} \tilde{q}(r)^{d+1}, \\ &\approx a \left(T_{\text{ECO}}^{d+1} - T_{\text{H}}^{d+1} \right) \Omega_{d-1} \int_{r=R_{\text{ECO}}}^{\Lambda} dr r_0^{d-1} \left(\frac{r_0}{(d-2)(r - \tilde{r}_0)} \right)^{\frac{d+1}{2}}, \\ &\approx a \left(T_{\text{ECO}}^{d+1} - T_{\text{H}}^{d+1} \right) \frac{2 \Omega_{d-1}}{(d-2)^{\frac{d+1}{2}} (d-1)} \frac{r_0^{\frac{3d-1}{2}}}{(R_{\text{ECO}} - \tilde{r}_0)^{\frac{d-1}{2}}}, \end{aligned} \quad (5.9)$$

where $\Lambda = 2r_0$ is the cutoff we had chosen for our thermal bath and where we are ignoring the energy of the outgoing modes at $r \gtrsim 2r_0$.

We will also be interested in the energy of a thin shell outside $r = R_{\text{ECO}}$. Note that the energy density (5.8) falls off as a power of $r - \tilde{r}_0$. We write

$$\Delta r \equiv R_{\text{ECO}} - \tilde{r}_0. \quad (5.10)$$

and define our thin shell as

$$R_{\text{ECO}} < r < R_{\text{ECO}} + \Delta r. \quad (5.11)$$

The energy of such a shell will be

$$E_{\text{rad}}^{\text{shell}} = \left(1 - \frac{1}{2^{\frac{d-1}{2}}}\right) E_{\text{rad}}. \quad (5.12)$$

It will be helpful to write

$$T_{\text{ECO}} = \eta_T T_H. \quad (5.13)$$

Noting the expression (3.5) for T_H , we then get

$$\begin{aligned} E_{\text{rad}} &= a \left(\eta_T^{d+1} - 1 \right) \frac{2(d-2)^{\frac{d+1}{2}} \Omega_{d-1}}{(4\pi)^{d+1} (d-1)} \frac{r_0^{\frac{d-3}{2}}}{(R_{\text{ECO}} - \tilde{r}_0)^{\frac{d-1}{2}}}, \\ &\equiv \frac{C_1 r_0^{\frac{d-3}{2}}}{(R_{\text{ECO}} - \tilde{r}_0)^{\frac{d-1}{2}}}, \end{aligned} \quad (5.14)$$

where C_1 is a dimensionless constant of order unity. Note that $C_1 > 0$ for $T_{\text{ECO}} > T_H$, and $C_1 < 0$ for $T_{\text{ECO}} < T_H$. We will have $C_1 = 0$ if $T_{\text{ECO}} = T_H$; i.e., $\eta_T = 1$. Our goal will be to show that this is the only allowed value for η_T for an ECO.

5.2 An outline of the argument

Let us first sketch the nature of the argument, before moving onto more detailed estimates. Let the spacetime be 3+1 dimensional for simplicity. We consider the cases $T_{\text{ECO}} < T_H$ and $T_{\text{ECO}} > T_H$ in turn.

5.2.1 The case $T_{\text{ECO}} < T_H$

Let us start with a simple case, depicted in fig. 3. Suppose $T_{\text{ECO}} = 0$. Suppose further that the ECO surface, which is at $r = R_{\text{ECO}}$, is only a Planck distance outside the horizon radius $r_0 = 2GM$; i.e., $s_{\text{ECO}} = l_p$ which gives $(R_{\text{ECO}} - \tilde{r}_0) \sim l_p^2/r_0$. The vacuum energy density outside R_{ECO} is negative and order Planck scale just outside the surface $r = R_{\text{ECO}}$. We find from (5.14)

$$E_{\text{rad}} \sim -\frac{1}{(R_{\text{ECO}} - \tilde{r}_0)} \sim -\frac{r_0}{l_p^2} \sim -M, \quad (5.15)$$

where we have used the fact that in 3+1 dimensions, $G = l_p^2$. Thus the vacuum energy outside the core of the ECO is negative and of the same order as the mass M seen at infinity.

For concreteness, let us assume that $E_{\text{rad}} = -\frac{1}{2}M$. Then from (5.1), we have

$$M(R_{\text{ECO}}) = M - E_{\text{rad}} = \frac{3}{2}M. \quad (5.16)$$

Now consider the validity of the relation (2.28) at $r = R_{\text{ECO}}$. Recall that $R_{\text{ECO}} \approx 2GM$. Thus we have

$$1 - \frac{2GM(R_{\text{ECO}})}{R_{\text{ECO}}} \approx 1 - \frac{3GM}{2GM} = -\frac{1}{2} < 0. \quad (5.17)$$

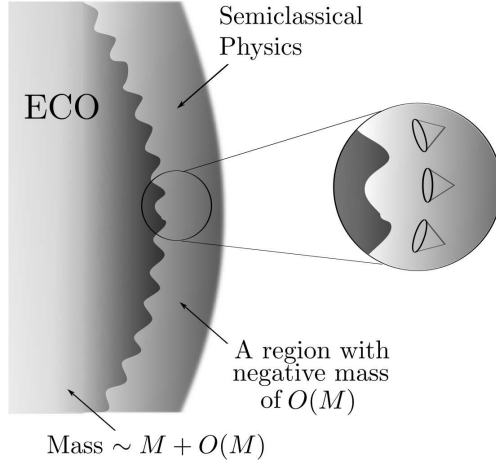


Figure 3: The argument for an ECO with $T_{\text{ECO}} < T_H$ and a surface $r = R_{\text{ECO}}$ that is just a Planck length outside the horizon radius. The region just outside R_{ECO} has a large negative energy density due to the negative vacuum energy. Thus the core of the ECO (the region depicted with a jagged boundary) must have a mass significantly more than M . Since the radius of this core is very close to the horizon radius r_0 for mass M , this core must be inside its own horizon; this fact is depicted in the magnified region by light cones that point inwards. Thus such an ECO cannot exist as a time-independent configuration.

This contradicts the requirement (2.28), which was required for regularity of the geometry.

Put another way, the vacuum energy outside the ECO contributes a negative value $-\frac{1}{2}M$ to the overall mass, which means the mass of the core has to be $\frac{3}{2}M$ to yield a total mass M at infinity. The Schwarzschild radius for this mass $\frac{3}{2}M$ is $3GM$, so that the core of the ECO is deep inside its own horizon radius. Recall that in classical general relativity, any particle inside a horizon must move towards smaller values of r by the inward pointing structure of light cones inside the horizon. Noting that semiclassical dynamics was required to hold at $r \geq R_{\text{ECO}}$, we conclude that the particles at the surface $r = R_{\text{ECO}}$ cannot stay at a fixed radius R_{ECO} ; instead, the core of the ECO must collapse. Thus we conclude that we cannot have such an ECO with $T_{\text{ECO}} = 0$.

The argument does not change in any significant way if we take some other temperature $T_{\text{ECO}} < T_H$. Suppose we take $T_{\text{ECO}} = \frac{1}{2}T_H$. Then $\eta_T = \frac{1}{2}$ in (5.13), as compared to the value $\eta_T = 0$ for the case $T_{\text{ECO}} = 0$. Using (5.14), we see that the energy $E_{\text{rad}}(\eta_T = \frac{1}{2})$ is smaller than $E_{\text{rad}}(\eta_T = 0)$ by a factor

$$\frac{E_{\text{rad}}(\eta_T = \frac{1}{2})}{E_{\text{rad}}(\eta_T = 0)} = \frac{1 - (\frac{1}{2})^4}{1} = \frac{15}{16}, \quad (5.18)$$

but this does not affect the nature of the argument we had outlined above for the case $T_{\text{ECO}} = 0$.

5.2.2 The case $T_{\text{ECO}} > T_H$

Now consider the case $T_{\text{ECO}} > T_H$, which is depicted in fig. 4. Condition ECO2 requires a high redshift at the surface R_{ECO} , which leads to a high local temperature for the radiation. Let us

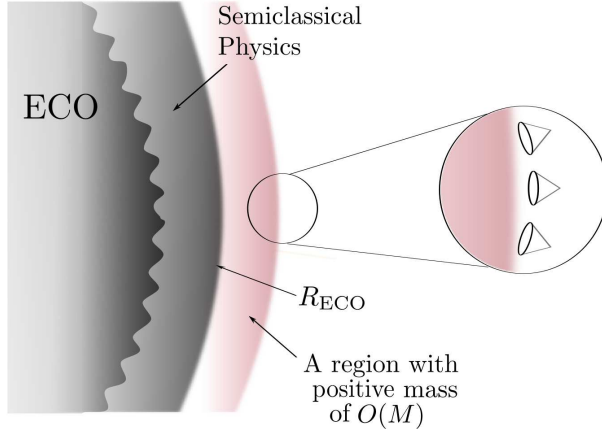


Figure 4: The argument for an ECO with $T_{\text{ECO}} > T_{\text{H}}$, and an surface at R_{ECO} where the redshift is very high. This high redshift implies that R_{ECO} is a very small distance outside the horizon radius \tilde{r}_0 corresponding to the mass inside R_{ECO} . The region just outside R_{ECO} has a large positive energy density due to the thermal radiation. A thin shell of this radiation, depicted as the outer band, has a significant amount of mass. Then the total mass in the region inside the outer boundary r_{outer} of this shell is such that the corresponding horizon radius $r_{0,\text{outer}}$ is larger than r_{outer} . Thus we again find that such an ECO cannot exist as a time-independent configuration.

assume for our example that this temperature is planck scale. Then the energy density at the ECO surface is also planck scale. The energy of radiation outside R_{ECO} is $E_{\text{rad}} \sim M$.

For concreteness, let us assume that $E_{\text{rad}} = \frac{1}{2}M$. Then the mass of the core of the ECO is $M(R_{\text{ECO}}) = \frac{1}{2}M$. Note that the horizon radius corresponding to this mass $M(R_{\text{ECO}})$ is $\tilde{r}_0 = GM$. Now we observe that in order to get the required high redshift at R_{ECO} , the mass inside R_{ECO} had to be compact enough to generate this high redshift. More precisely, we need the surface R_{ECO} to be $\sim l_p$ outside the radius $\tilde{r}_0 = GM$; thus we write $R_{\text{ECO}} \approx GM$.

Now consider a shell of radiation, with width l_p , just outside the ECO surface. Thus the outer boundary of this shell r_{outer} is very close to R_{ECO} , which was very close to $\tilde{r}_0 = GM$. Thus $r_{\text{outer}} \approx GM$.

By (5.12), the energy of the shell is $E_{\text{rad}}^{\text{shell}} = \frac{1}{2}E_{\text{rad}} = 0.25M$. Thus the total mass inside the radius r_{outer} is $M(r_{\text{outer}}) = 0.5M + 0.25M = 0.75M$. Now consider the validity of the relation (2.28) at $r = R_{\text{ECO}}$. We have

$$1 - \frac{2GM(r_{\text{outer}})}{r_{\text{outer}}} \approx 1 - \frac{1.5GM}{GM} = -0.5 < 0, \quad (5.19)$$

which contradicts the requirement (2.28).

In other words, the core of the ECO had to be very compact to yield a high redshift at R_{ECO} . We then find that a thin shell just outside this core adds enough mass so that the system given by core+shell is inside its own horizon radius; thus such an ECO cannot exist.

5.3 Defining a useful scale Δr_{crit}

Let us review the quantities which played a role in the above arguments. The difference $r_0 - \tilde{r}_0$ described the difference between the Schwarzschild radius r_0 for the mass M of the ECO, and the Schwarzschild radius \tilde{r}_0 of the core of the ECO. This difference stems from the fact that a part E_{rad} of the mass M of the ECO is carried by the radiation surrounding the core of the ECO. The energy E_{rad} in turn depends on

$$\Delta r \equiv (R_{\text{ECO}} - \tilde{r}_0). \quad (5.20)$$

A very small value of $(R_{\text{ECO}} - \tilde{r}_0)$ gives a very large E_{rad} and thus a very large $r_0 - \tilde{r}_0$. Conversely, a very large $(R_{\text{ECO}} - \tilde{r}_0)$ gives a very small E_{rad} and thus a very small $r_0 - \tilde{r}_0$.

Given the above, it will be useful to define a critical value Δr_{crit} for $R_{\text{ECO}} - \tilde{r}_0$, such the corresponding radiation energy E_{rad} shifts the horizon radius by an amount which is again $r_0 - \tilde{r}_0 = \Delta r_{crit}$. Recalling that the horizon radius satisfies $r_0^{d-2} = \mu GM$, we note that small shifts of this radius are given by $\delta r_0 \approx \frac{\mu G \delta M}{(d-2)r_0^{d-3}}$. Setting $\delta M = -E_{rad}$, we find that

$$|r_0 - \tilde{r}_0| \approx \frac{\mu G |E_{rad}|}{(d-2)r_0^{d-3}} \approx \frac{\mu G |C_1|}{(\Delta r)^{\frac{d-1}{2}} (d-2)r_0^{\frac{d-3}{2}}}, \quad (5.21)$$

where we have used the expression for E_{rad} from (5.14). We define the critical separation Δr_{crit} as the value of Δr when this shift $|r_0 - \tilde{r}_0|$ equals Δr defined in (5.20). Thus we have

$$\Delta r_{crit} = \frac{\mu G |C_1|}{(\Delta r_{crit})^{\frac{d-1}{2}} (d-2) r_0^{\frac{d-3}{2}}}. \quad (5.22)$$

which gives

$$\Delta r_{crit} = \left(\frac{\mu G |C_1|}{(d-2) r_0^{\frac{d-3}{2}}} \right)^{\frac{2}{d+1}}. \quad (5.23)$$

To get an idea of the scale Δr_{crit} , we write it in terms of a proper distance s_{crit} using the relation (2.8) between coordinate distance from the horizon and proper distance from the horizon. Then we get

$$s_{crit} \sim \left(\frac{M}{m_p} \right)^{\frac{2}{(d-2)(d+1)}} l_p \sim s_c, \quad (5.24)$$

where the compactness scale s_c was defined in (2.12).

5.4 The argument for $T_{\text{ECO}} < T_{\text{H}}$

Let us assume that $T_{\text{ECO}} < T_{\text{H}}$, so that $\eta_{\text{T}} < 1$. As noted above, a crucial role in the argument is played by the quantity $\Delta r = R_{\text{ECO}} - \tilde{r}_0$. We will consider separately the following two possibilities:

(a) $\Delta r \ll \Delta r_{crit}$:

Since $\eta_T < 1$, we have $E_{\text{rad}} < 0$. Further,

$$|E_{\text{rad}}| = \frac{|C_1| r_0^{\frac{d-3}{2}}}{(R_{\text{ECO}} - \tilde{r}_0)^{\frac{d-1}{2}}} \gg \frac{|C_1| r_0^{\frac{d-3}{2}}}{(\Delta r_{\text{crit}})^{\frac{d-1}{2}}}. \quad (5.25)$$

Since $E_{\text{rad}} < 0$, we have $\tilde{r}_0 > r_0$. From (5.21) we have

$$(\tilde{r}_0 - r_0) = \frac{\mu G |E_{\text{rad}}|}{(d-2) r_0^{d-3}} \gg \frac{\mu G |C_1|}{(\Delta r_{\text{crit}})^{\frac{d-1}{2}} (d-2) r_0^{\frac{d-3}{2}}} \sim \Delta r_{\text{crit}}, \quad (5.26)$$

where the last relation follows from using the definition (5.22) of Δr_{crit} .

Now, since $R_{\text{ECO}} > \tilde{r}_0$, we find that

$$R_{\text{ECO}} - r_0 = (R_{\text{ECO}} - \tilde{r}_0) + (\tilde{r}_0 - r_0) > (\tilde{r}_0 - r_0) \gg \Delta r_{\text{crit}}, \quad (5.27)$$

where in the last step we have used (5.26). Given that the separation Δr_{crit} corresponds to the proper distance scale s_c by (5.24), we see that our ECO is not sufficiently compact to satisfy condition ECO1.

(b) $\Delta r \gtrsim \Delta r_{\text{crit}}$:

In this situation the redshift at the ECO surface is, using (2.14)

$$q(R_{\text{ECO}}) \approx \frac{r_0^{\frac{1}{2}}}{(d-2)^{\frac{1}{2}} (R_{\text{ECO}} - \tilde{r}_0)^{\frac{1}{2}}} \lesssim \frac{r_0^{\frac{1}{2}}}{(\Delta r_{\text{crit}})^{\frac{1}{2}}} \sim \left(\frac{r_0}{l_p} \right)^{\frac{d-1}{d+1}}. \quad (5.28)$$

This violates the condition ECO2 (eq. (2.16)) which requires that we have a higher redshift than (5.28) at R_{ECO} .

Thus we find that for $T_{\text{ECO}} < T_{\text{H}}$, we cannot get an ECO satisfying the conditions ECO1-ECO3.

5.5 The estimate for $T_{\text{ECO}} > T_{\text{H}}$

Now we consider the case $T_{\text{ECO}} > T_{\text{H}}$, so that $\eta_T > 1$. Again we proceed to examine the two possibilities:

(a) $\Delta r \ll \Delta r_{\text{crit}}$:

Since $\eta_T > 1$, we have $E_{\text{rad}} > 0$. Further,

$$E_{\text{rad}} = \frac{C_1 r_0^{\frac{d-3}{2}}}{(R_{\text{ECO}} - \tilde{r}_0)^{\frac{d-1}{2}}} \gg \frac{C_1 r_0^{\frac{d-3}{2}}}{(\Delta r_{\text{crit}})^{\frac{d-1}{2}}}. \quad (5.29)$$

Since $E_{\text{rad}} > 0$, we have $r_0 > \tilde{r}_0$, and

$$(r_0 - \tilde{r}_0) = \frac{\mu G E_{\text{rad}}}{(d-2) r_0^{d-3}} \gg \frac{\mu G |C_1|}{(\Delta r_{\text{crit}})^{\frac{d-1}{2}} (d-2) r_0^{\frac{d-3}{2}}} \sim \Delta r_{\text{crit}}. \quad (5.30)$$

Now consider the thin shell outside $r = R_{\text{ECO}}$ with coordinate width Δr as defined in (5.11). We have from (5.12)

$$E_{\text{rad}}^{\text{shell}} = \left(1 - \frac{1}{2^{\frac{d-1}{2}}}\right) \frac{C_1 r_0^{\frac{d-3}{2}}}{(R_{\text{ECO}} - \tilde{r}_0)^{\frac{d-1}{2}}} \gg \frac{C_1 r_0^{\frac{d-3}{2}}}{(\Delta r_{\text{crit}})^{\frac{d-1}{2}}}. \quad (5.31)$$

Let us define $\tilde{r}_{0,\text{outer}}$ as the Schwarzschild radius corresponding to the mass within radius r_{outer} ; i.e., we define $r_{0,\text{outer}}$ through the condition $r_{0,\text{outer}}^{d-2} \equiv \mu GM(r_{\text{outer}})$. Then we have

$$r_{0,\text{outer}} - \tilde{r}_0 \approx \frac{\mu G E_{\text{rad}}^{\text{shell}}}{(d-2)r_0^{d-3}} \gg \frac{\mu G |C_1|}{(\Delta r_{\text{crit}})^{\frac{d-1}{2}} (d-2) r_0^{\frac{d-3}{2}}} \sim \Delta r_{\text{crit}}, \quad (5.32)$$

where in the last step we have used (5.22). Now recall that we had chosen the coordinate width of the shell as described in (5.11), which says

$$r_{\text{outer}} - R_{\text{ECO}} = R_{\text{ECO}} - \tilde{r}_0. \quad (5.33)$$

Thus since $\Delta r = (R_{\text{ECO}} - \tilde{r}_0) \ll \Delta r_{\text{crit}}$, we find

$$r_{\text{outer}} - R_{\text{ECO}} \ll \Delta r_{\text{crit}}. \quad (5.34)$$

On the other hand, from (5.32) we have

$$r_{0,\text{outer}} - \tilde{r}_0 \gg \Delta r_{\text{crit}}. \quad (5.35)$$

Subtracting (5.34) from (5.35) we get

$$(r_{0,\text{outer}} - r_{\text{outer}}) + (R_{\text{ECO}} - \tilde{r}_0) \gg \Delta r_{\text{crit}}. \quad (5.36)$$

Again using $(R_{\text{ECO}} - \tilde{r}_0) \ll \Delta r_{\text{crit}}$ we find

$$(r_{0,\text{outer}} - r_{\text{outer}}) \gg \Delta r_{\text{crit}}. \quad (5.37)$$

Thus we find that

$$r_{\text{outer}} < r_{0,\text{outer}}. \quad (5.38)$$

This is a violation of equation (2.11), since it implies

$$1 - \frac{\mu GM(r_{\text{outer}})}{r_{\text{outer}}^{d-2}} = 1 - \frac{r_{0,\text{outer}}^{d-2}}{r_{\text{outer}}^{d-2}} < 0. \quad (5.39)$$

(b) $\Delta r \gtrsim \Delta r_{\text{crit}}$:

The argument here will be the same as the one for the case $T_{\text{ECO}} < T_{\text{H}}$. The redshift at the ECO surface is, using (2.14)

$$q(R_{\text{ECO}}) \approx \frac{r_0^{\frac{1}{2}}}{(d-2)^{\frac{1}{2}}(R_{\text{ECO}} - \tilde{r}_0)^{\frac{1}{2}}} \lesssim \frac{r_0^{\frac{1}{2}}}{(\Delta r_{\text{crit}})^{\frac{1}{2}}} \sim \left(\frac{r_0}{l_p}\right)^{\frac{d-1}{d+1}}. \quad (5.40)$$

This violates the condition ECO2 (eq. (2.16)) which requires that we have a higher redshift at R_{ECO} .

Thus we find that for $T_{\text{ECO}} > T_{\text{H}}$, we cannot get an ECO satisfying the conditions ECO1-ECO3.

6 Using the Tolman-Oppenheimer-Volkoff equation

In the analysis of the previous section, we ignored the feedback of the radiation on the metric. In this section we will make a more self-consistent analysis of the field equations near the surface $r = R_{\text{ECO}}$.

We have taken our metric to be described by the spherically symmetric ansatz (2.4) in the region $r > R_{\text{ECO}}$. In the near surface region the local temperature is very high, due to the large redshift required by condition ECO2. Thus a typical quantum field with mass $m \ll m_p$ will appear massless to leading order. We will assume the stress tensor of the thermal gas near the ECO surface to have the form of a perfect fluid. With the directions of the orthonormal frame in aligned along t, r , and the angular directions. we have

$$T^\mu_\nu{}^{\text{radiation}} = \text{diag}\{-\rho^r(r), p^r(r), p^r(r), \dots, p^r(r)\}, \quad (6.1)$$

where $\rho^r(r)$ and $p^r(r)$ denote the density and pressure of the radiation respectively. Due to the large redshift factor in this region and the correspondingly high local temperature, we choose the equation of state

$$p^r(r) = \frac{1}{d}\rho^r(r), \quad (6.2)$$

appropriate to a massless field.

In the vacuum black hole geometry, in the high redshift region near $r = r_0$, the vacuum energy near the horizon also has the form (6.1),(6.2). One can see this from the picture of the near horizon Boulware vacuum as the Rindler vacuum; the vacuum stress-tensor of this Rindler vacuum is the negative of the stress tensor of a thermal gas at temperature $T = \frac{1}{2\pi s}$, and such a thermal gas satisfies (6.1),(6.2).

Recall from the discussion of section 3 that vacuum energy near the ECO surface has the same order of magnitude as the energy density of thermal quanta. We will assume that the vacuum energy just outside $r = R_{\text{ECO}}$ also has a form like (6.1),(6.2)

$$T^\mu_\nu{}^{\text{vacuum}} = \text{diag}\{-\rho^v(r), p^v(r), p^v(r), \dots, p^v(r)\}, \quad (6.3)$$

where $\rho^v(r)$ and $p^v(r)$ denote the density and pressure of the vacuum respectively. Further we assume

$$p^v = \frac{1}{d}\rho^v. \quad (6.4)$$

We cannot provide a rigorous justification for this assumption, but we will give arguments to make it plausible. Since the metric outside the ECO is not the metric of a black hole, a priori we have to solve the analog of equation (3.11) for the field modes in the ECO geometry, and then compute the vacuum stress energy from those modes. This is a difficult computation, and so we assume (6.3) as a heuristic extrapolation motivated by the properties of the vacuum stress tensor in the black hole geometry. It is important to note that we are not specifying the *value* of $\rho^v(r)$ for the vacuum stress tensor; we are just assuming that the vacuum energy stress tensor is diagonal, isotropic and traceless. In the next section we will work with the 1+1 dimensional system, where we will know the vacuum energy explicitly in the fully backreacted geometry of the ECO. For now we just check that (6.3) is consistent to leading order with the requirements of the vacuum stress tensor.

Consider for example a massless scalar field in 3+1 dimensions. The anomaly $\langle T^\mu{}_\mu \rangle$ has terms which are order curvature squared; e.g., we have a term $R^{\mu\nu}R_{\mu\nu}$ with coefficient of order unity (see for example [41]). From Einstein's equations $G_{\mu\nu} = 8\pi GT_{\mu\nu}$, we see that

$$R^{\mu\nu}R_{\mu\nu} \sim G^2\rho^2. \quad (6.5)$$

We compare this contribution to $\langle T^\mu{}_\mu \rangle$ to the component ρ of the stress tensor, finding

$$\frac{G^2\rho^2}{\rho} \sim G^2\rho \sim l_p^4 T^4 \sim \frac{l_p^4}{s^4}, \quad (6.6)$$

where we have noted that the temperature $T_{\text{ECO}}(r)$ of the ECO at a proper distance s from the horizon radius goes like $T \sim \frac{1}{s}$. (Recall that we are always assuming that $T_{\text{ECO}} \sim T_{\text{H}}$.) So, as long as we look at distances $s \gg l_p$, this contribution to the trace $\langle T^\mu{}_\mu \rangle$ is much smaller than the components ρ^v, p^v of the stress tensor.

Similar arguments give bounds on other contributions to the anomaly $\langle T^\mu{}_\mu \rangle$. For example

$$\square R \sim \frac{1}{s^2} GT^\mu{}_\mu \lesssim \frac{G\rho}{s^2} \sim \frac{l_p^2}{s^6}, \quad (6.7)$$

Here we have replaced the derivatives in \square with $1/s^2$, with s being the scale over which all quantities vary in the near horizon region, and in the second step used the fact that the trace $T^\mu{}_\mu$ must be less than or order ρ . Again we find

$$\frac{\square R}{\rho} \lesssim \frac{l_p^2}{s^2}, \quad (6.8)$$

which is small for $s \gg l_p$.

We therefore see that it is consistent to assume a traceless vacuum stress tensor to leading order, as encoded in the condition (6.4). Assuming (6.3), (6.4) for the vacuum stress energy, the total stress energy (radiation +vacuum) in the near-surface region also has the form

$$T^\mu{}_\nu = \text{diag}\{-\rho(r), p(r), p(r), \dots, p(r)\}, \quad (6.9)$$

with the pressure

$$p = \frac{1}{d}\rho. \quad (6.10)$$

Our goal now is to solve the Tolman-Oppenheimer-Volkoff (TOV) equations with such a stress tensor in the region just outside $r = R_{\text{ECO}}$.

6.1 Approximating the TOV equation

From the estimates in section 5, we note that we are interested in the situation where the stress tensor in the region $r > R_{\text{ECO}}$ falls off rapidly with increasing $r - r_0$. Since R_{ECO} is very close to the value r_0 , we will be able to use the approximation

$$r \approx r_0. \quad (6.11)$$

in many of the terms in the TOV equation. This approximation will allow us to simplify the equation. We will find that this approximate equation has no solution which yields an ECO. We will then re-examine the approximations we made in simplifying the TOV equation, and find that these approximations become invalid only when we are outside the compactness scale s_c defined in (2.12). Thus we will conclude that if an ECO satisfies condition ECO1, then there must be vanishing (at leading order) of the stress tensor (6.9) at $r > R_{\text{ECO}}$. As we saw in section 3, the vanishing of this stress tensor happens when $T_{\text{ECO}} = T_{\text{H}}$ and the geometry in the region just outside $r > R_{\text{ECO}}$ becomes the geometry of the traditional black hole with a vacuum around the horizon.

Before proceeding to obtain the approximate form of the TOV equation valid near $r \approx r_0$, we note what is known about the exact TOV equation, for the case where the stress tensor is given by (6.9), (6.10). The Einstein equations can be reduced to a single nonlinear second order equation called the Emden-Chandrasekhar equation [42]. This equation has an analytically known solution which is singular at the origin. For the 3 + 1 dimensional case, the solution has the form.

$$\rho = \frac{Q_1}{r^2}, \quad e^{2\alpha} = Q_2 r, \quad e^{2\beta} = Q_3, \quad (6.12)$$

where Q_i are positive constants. The solution regular at the origin cannot be solved for analytically, but its asymptotic form has been developed as a power series. The singular solution is discarded when we consider the context of stellar structure, where the ‘truncated isothermal sphere’ can be used to model the core of a star. In our problem, we have the opposite situation, where the region $r < R_{\text{ECO}}$ is a quantum gravitational region *not* described by isothermal semiclassical physics, while the region $r > R_{\text{ECO}}$ can take the form of an isothermal region, truncated at some radius r_{max} . Thus the singular solution (6.12) is also an allowed solution in the region $R_{\text{ECO}} < r < r_{\text{max}}$.

This singular solution shows the relevance of our condition ECO3, which says that there should not be too much matter far from the ECO surface. Take the singular isothermal solution (6.12), truncated at some large radius R . Choose a small radius $r = \epsilon$, and replace the singular region in its interior by some unspecified quantum dynamics. Now if we let $R_{\text{ECO}} = \epsilon$, we see that, formally, such a solution will satisfy the conditions ECO1, ECO2. Condition ECO1 says that r_{ECO} be not much larger than r_0 , and here we have $R_{\text{ECO}} = \epsilon \ll r_0$. Condition ECO2 requires a high redshift at $r = R_{\text{ECO}}$, and from (6.12) we see that $q(\epsilon) = e^{-\beta(\epsilon)}$ is indeed large. But note that almost all the mass of this object is outside $r = R_{\text{ECO}}$. To exclude such a case from our analysis we had imposed the condition ECO3.

While we cannot solve the isothermal TOV equation exactly, we will find that we have a high energy density in the region very close to $r = r_0$. In this situation we can get an approximation to the TOV equation that we can solve in closed form, and this solution will yield a more rigorous derivation of the heuristic estimates of section 5.

6.1.1 Preliminary steps

For the metric ansatz (2.4), the conservation law $T^{r\mu}_{;\mu} = 0$ gives

$$\alpha' = -\frac{p'}{p + \rho}, \quad (6.13)$$

where a prime denotes $\frac{d}{dr}$. Setting $p = \frac{\rho}{d}$ from (6.10) gives us

$$\alpha' = -\frac{1}{(d+1)} \frac{\rho'}{\rho}. \quad (6.14)$$

The solution to this equation is

$$e^{2\alpha} = \frac{C_2}{|\rho|^{\frac{2}{d+1}}}, \quad (6.15)$$

where $C_2 > 0$ is a constant.

The Einstein equation $G_{tt} = 8\pi GT_{tt}$ gives the g_{rr} coefficient $e^{2\beta(r)}$ through (2.26), (2.27). From (2.27) we find

$$M'(r) = \Omega_{d-1} r^{d-1} \rho(r). \quad (6.16)$$

With the approximation (6.11), this becomes

$$M'(r) \approx \Omega_{d-1} r_0^{d-1} \rho(r). \quad (6.17)$$

6.1.2 Approximating the TOV equation

The TOV equation in $d+1$ dimensions reads

$$r^{d-1} p'(r) = -\frac{(d-2)\mu}{2} GM(r) \rho(r) \left(1 + \frac{p(r)}{\rho(r)}\right) \left(1 + \frac{16\pi p(r) r^d}{\mu(d-2)(d-1)M(r)}\right) \left(1 - \frac{\mu GM(r)}{r^{d-2}}\right)^{-1}. \quad (6.18)$$

We simplify this equation using the approximation (6.11):

(a) Using our assumed equation of state $p = \frac{1}{d}\rho$ we get

$$-r^{d-1} p'(r) = -\frac{1}{d} r^{d-1} \rho'(r) \approx -\frac{1}{d} r_0^{d-1} \rho'(r). \quad (6.19)$$

(b) We have

$$1 + \frac{p(r)}{\rho(r)} = \frac{d+1}{d}. \quad (6.20)$$

(c) We have

$$1 + \frac{16\pi p(r) r^d}{\mu(d-2)(d-1)M(r)} = 1 + \frac{16\pi \rho(r) r^d}{\mu d(d-2)(d-1)M(r)} \approx 1 + \frac{16\pi \rho(r) r_0^d}{\mu d(d-2)(d-1)M(r)}. \quad (6.21)$$

We also note that if we were to distribute a mass M uniformly over a radius r_0 , we would get a density

$$\rho_{\text{uniform}} \sim \frac{M}{r_0^d}. \quad (6.22)$$

By contrast, in the example of section 5.2, we had taken $\text{SECO} \sim l_p$, and found that the energy of radiation in a planck width shell was also order $\sim M$. So, in that example the energy density $\rho(r)$ near the ECO would be higher than ρ_{uniform} by a factor $r_0/l_p \gg 1$.

More generally, we assume that the energy density near the surface of the ECO is much higher than ρ_{uniform} , which implies that

$$p \sim \rho \gg \frac{M}{r_0^d}. \quad (6.23)$$

Thus we make the approximation

$$1 + \frac{16\pi\rho(r) r_0^d}{\mu d(d-2)(d-1)M(r)} \approx \frac{16\pi\rho(r) r_0^d}{\mu d(d-2)(d-1)M(r)}. \quad (6.24)$$

(d) We have

$$\left(1 - \frac{\mu GM(r)}{r_0^{d-2}}\right)^{-1} \approx \left(1 - \frac{\mu GM(r)}{r_0^{d-2}}\right)^{-1}. \quad (6.25)$$

With these approximations, and using (6.17) to express ρ , the TOV equation (6.18) reduces to

$$\left(1 - \frac{\mu GM(r)}{r_0^{d-2}}\right)M''(r) = -\frac{\mu G}{2r_0^{d-2}} \frac{(d+1)}{d} (M'(r))^2, \quad (6.26)$$

In what follows we will call this the approximate TOV equation.

6.1.3 Solving the approximate TOV equation

Let us write

$$u(r) = 1 - \frac{\mu GM(r)}{r_0^{d-2}}. \quad (6.27)$$

Then (6.26) becomes

$$u(r)u''(r) = \frac{(d+1)}{2d} (u'(r))^2. \quad (6.28)$$

The solution to this equation is

$$u'(r) = C_3 u(r)^{\frac{d+1}{2d}}, \quad (6.29)$$

and a final integration gives

$$u(r) = \left(\frac{(d-1)}{2d} C_3 (r - r_1) \right)^{\frac{2d}{d-1}}. \quad (6.30)$$

Thus we have

$$1 - \frac{\mu GM(r)}{r_0^{d-2}} = \left(\frac{(d-1)}{2d} C_3 (r - r_1) \right)^{\frac{2d}{d-1}}. \quad (6.31)$$

6.1.4 Range of validity of the approximation

We have obtained the approximate TOV equation (6.26) for the near-surface region of the ECO. This approximation will be good for a range

$$R_{\text{ECO}} < r \lesssim r_{\max}. \quad (6.32)$$

We will now obtain an estimate for r_{\max} .

1. Recall that in eq. (6.23) we had set

$$\frac{p(r)r_0^d}{M(r)} \gg 1. \quad (6.33)$$

This inequality is expected to hold close to the ECO surface, since $p(r) \sim \rho(r) \sim T_{\text{ECO}}^{d+1}(r) \sim T_{\text{H}}^{d+1}(r)$, and $T_{\text{H}}(r)$ is large near the ECO surface due to the large redshift $q(r)$.

To get a rough estimate of scales, we use the expression (2.14) for $q(r)$ for the black hole geometry to get

$$p(r) \sim T_{\text{H}}^{d+1} q(r)^{d+1} \sim \frac{1}{r_0^{d+1}} \left(\frac{r_0}{r - r_0} \right)^{\frac{d+1}{2}} \sim \frac{1}{r_0^{\frac{d+1}{2}} (r - r_0)^{\frac{d+1}{2}}}. \quad (6.34)$$

We also have

$$M(r) \sim M \sim \frac{r_0^{d-2}}{G} = \frac{r_0^{d-2}}{l_p^{d-1}}. \quad (6.35)$$

Thus,

$$\frac{p(r)r_0^d}{M(r)} \sim \frac{l_p^{d-1}}{(r - r_0)^{\frac{d+1}{2}} r_0^{\frac{d-3}{2}}}. \quad (6.36)$$

We find that $\frac{p(r)r_0^d}{M(r)} \sim 1$ at

$$(r - r_0) \sim \left(\frac{l_p^{d-1}}{r_0^{\frac{d-3}{2}}} \right)^{\frac{2}{d+1}}. \quad (6.37)$$

Using the relation (2.8) to write this value of $r - r_0$ in terms of the proper distance s from r_0 in the black hole metric, we find

$$s \sim M^{\frac{2}{(d-2)(d+1)}} l_p. \quad (6.38)$$

Thus, we find that for the condition (6.33) to hold, the value of r_{\max} defined in (6.32) is given by the same distance scale s_c (eq. (2.12)) that was used to define the compactness of the ECO in condition ECO1.

2. In (6.26) we needed to evaluate the derivative of $\frac{M(r)}{r}$, but we approximated this by the derivative of $\frac{M(r)}{r_0}$; thus we were ignoring the variation of the value of r in the near surface region. Writing

$$\frac{d}{dr} \left(\frac{M(r)}{r} \right) = \frac{1}{r} \frac{dM(r)}{dr} - \frac{M(r)}{r^2}, \quad (6.39)$$

we see that this approximation is valid as long as the ratio between the two terms on the RHS satisfies

$$z(r) \equiv \left(\frac{M(r)}{r^2} \right) \left(\frac{1}{r} \frac{dM(r)}{dr} \right)^{-1} \ll 1. \quad (6.40)$$

Using (6.16) and the same estimates for $\rho(r)$ that we used for $p(r)$ in (6.34), we find

$$z(r) \sim \frac{(r - r_0)^{\frac{d+1}{2}} M}{r_0^{\frac{d-1}{2}}}. \quad (6.41)$$

Thus $z(r) \sim 1$ at

$$(r - r_0) \sim \left(\frac{r_0^{\frac{d-1}{2}}}{M} \right)^{\frac{2}{d+1}} \sim \left(\frac{l_p^{d-1}}{r_0^{\frac{d-3}{2}}} \right)^{\frac{2}{d+1}}. \quad (6.42)$$

This is the same distance scale that appeared (6.37), so we again find that r_{max} is the radius given by the compactness scale s_c .

Thus in the discussion below, we will set

$$r_{max} - r_0 = \left(\frac{l_p^{d-1}}{r_0^{\frac{d-3}{2}}} \right)^{\frac{2}{d+1}}. \quad (6.43)$$

Since the radius $r \sim r_{max}$ is at the compactness scale s_c , we see by condition ECO3 that the redshift factor at r_{max} must be of the same order as the redshift factor predicted by the black hole geometry. Thus

$$q(r_{max}) \sim \left(\frac{r_0}{l_p} \right)^{\frac{d-1}{d+1}} \sim \left(\frac{M}{m_p} \right)^{\frac{(d-1)}{(d-2)(d+1)}}. \quad (6.44)$$

6.2 Analyzing the approximate TOV solution

First, consider the power $\frac{2d}{d-1}$ appearing on the RHS of (6.31). We are considering $d \geq 3$. For $d = 3$, this power is an odd integer 3, while for all higher d it is a fraction. The LHS of (6.31) must be a positive real number by the requirement (2.28), so we need

$$C_3(r - r_1) > 0, \quad (6.45)$$

throughout the domain (6.32) where our approximate solution is valid. This gives us two possibilities, which we study in turn.

6.2.1 The case $C_3 > 0, r_1 < R_{\text{ECO}}$:

One possibility is that we have $C_3 > 0$, and $r_1 < R_{\text{ECO}}$, which gives (6.45) throughout the domain (6.32). Using (6.31) we find

$$\rho(r) = -\frac{d}{8\pi Gr_0} \left(\frac{(d-1)}{2d} |C_3| \right)^{\frac{2d}{d-1}} (r - r_1)^{\frac{d+1}{d-1}}. \quad (6.46)$$

We see that $\rho(r) < 0$. Thus this situation is similar to the case $T_{\text{ECO}} < T_{\text{H}}$ which had $\rho(r) < 0$ in our heuristic analysis of section 5. From (6.15) we find

$$e^{2\alpha(r)} = \frac{C_2}{|\rho|^{\frac{2}{d+1}}} = C_2 \left(\frac{d}{8\pi Gr_0} \left(\frac{(d-1)}{2d} |C_3| \right)^{\frac{2d}{d-1}} \right)^{-\frac{2}{d+1}} (r - r_1)^{-\frac{2}{(d-1)}}. \quad (6.47)$$

Note that $e^{2\alpha(r)}$ determines the redshift factor

$$q(r) = (-g_{tt}(r))^{-\frac{1}{2}} = e^{-\alpha(r)} = C_2^{-\frac{1}{2}} \left(\frac{d}{8\pi Gr_0} \left(\frac{(d-1)}{2d} |C_3| \right)^{\frac{2d}{d-1}} \right)^{\frac{1}{d+1}} (r - r_1)^{\frac{1}{d-1}}. \quad (6.48)$$

We see that since $r > r_1$, the redshift factor $q(r)$ *increases* as we move r to larger values. Thus $q(r)$ will keep increasing monotonically until at least the location $r = r_{\text{max}}$ where our near-surface approximation (6.11) to the TOV equation fails. Thus

$$q(R_{\text{ECO}}) < q(r_{\text{max}}) \sim \left(\frac{M}{m_p} \right)^{\frac{(d-1)}{(d-2)(d+1)}}, \quad (6.49)$$

where in the second step we have recalled (6.44). Thus we see that we do not satisfy the high redshift condition (2.16).

6.2.2 The case $C_3 < 0, r_1 > R_{\text{ECO}}$:

Now consider the possibility that

$$C_3 < 0, \quad r_1 > R_{\text{ECO}}. \quad (6.50)$$

We write $\rho(r)$ as

$$\rho(r) = \frac{d}{8\pi Gr_0} \left(\frac{(d-1)}{2d} |C_3| \right)^{\frac{2d}{d-1}} (r_1 - r)^{\frac{d+1}{d-1}}. \quad (6.51)$$

We see that $\rho(r) > 0$. Thus this situation is similar to the case $T_{\text{ECO}} > T_{\text{H}}$ which had $\rho(r) > 0$ in our heuristic analysis of section 5.

Note that the LHS of (6.31) is required to not vanish anywhere, but the RHS vanishes at $r = r_1$. We avoid an inconsistency only if r_1 is sufficiently large that values $r \approx r_1$ lie outside the range where the near-surface approximation (6.11) of the TOV equation is valid. Recall that r_{max} is the same order as the compactness scale s_c , and that outside this compactness scale the standard black hole geometry is expected to be a reasonable approximation to the

geometry. Noting that the solution (6.31) is a power law in the near-surface region, we state the requirement that r_1 be significantly outside the range $r_0 < r < r_{max}$ by requiring

$$r_1 - r_{max} \gtrsim r_{max} - r_0. \quad (6.52)$$

Even though we say that r_1 is far outside the compactness scale s_c , we will take $r_1 - r_0 \ll r_0$, and will use this approximation to simplify some relations; taking a larger r_1 does not change the argument that follows.

Again, using (6.15) we have

$$q(r) = (-g_{tt}(r))^{\frac{1}{2}} = e^{-\alpha(r)} = C_2^{-\frac{1}{2}} \left(\frac{d}{8\pi G r_0} \left(\frac{(d-1)}{2d} |C_3| \right)^{\frac{2d}{d-1}} \right)^{\frac{1}{d+1}} (r_1 - r)^{\frac{1}{d-1}}. \quad (6.53)$$

In the standard black hole geometry,

$$q(r) \approx \left(\frac{(d-2)(r - r_0)}{r_0} \right)^{-\frac{1}{2}}. \quad (6.54)$$

The expression (6.53) holds for $R \lesssim r_{max}$ while by condition ECO3, the expression (6.54) holds for $r \gtrsim r_{max}$. Thus at $r \sim r_{max}$ both expressions should have approximately the same value. Thus we must have

$$C_2^{-\frac{1}{2}} \left(\frac{d}{8\pi G r_0} \left(\frac{(d-1)}{2d} |C_3| \right)^{\frac{2d}{d-1}} \right)^{\frac{1}{d+1}} (r_1 - r_{max})^{\frac{1}{d-1}} \approx \left(\frac{(d-2)(r_{max} - r_0)}{r_0} \right)^{-\frac{1}{2}}. \quad (6.55)$$

Thus the constants C_2, C_3 in the above relation satisfy

$$C_2^{-\frac{1}{2}} \left(\frac{d}{8\pi G r_0} \left(\frac{(d-1)}{2d} |C_3| \right)^{\frac{2d}{d-1}} \right)^{\frac{1}{d+1}} \approx \left(\frac{r_0}{(d-2)(r_{max} - r_0)} \right)^{\frac{1}{2}} \frac{1}{(r_1 - r_{max})^{\frac{1}{d-1}}}. \quad (6.56)$$

Then the redshift at $r = R_{\text{ECO}}$ is given by (using eq.(6.53))

$$q(R_{\text{ECO}}) \approx \left(\frac{r_0}{(d-2)(r_{max} - r_0)} \right)^{\frac{1}{2}} \left(\frac{r_1 - R_{\text{ECO}}}{r_1 - r_{max}} \right)^{\frac{1}{d-1}}. \quad (6.57)$$

We now wish to use the intuition that r_1 is ‘large’ in the sense (6.52). We have

$$\frac{r_1 - R_{\text{ECO}}}{r_1 - r_{max}} = 1 + \frac{r_{max} - R_{\text{ECO}}}{r_1 - r_{max}} < 1 + \frac{r_{max} - r_0}{r_1 - r_{max}} < 1 + \frac{r_{max} - r_0}{r_{max} - r_0} = 2, \quad (6.58)$$

where in the last step we have used the relation $(r_1 - r_{max}) \gtrsim (r_{max} - r_0)$. Then (6.57) gives

$$q(R_{\text{ECO}}) \sim \left(\frac{r_0}{(d-2)(r_{max} - r_0)} \right)^{\frac{1}{2}} \sim \left(\frac{r_0}{l_p} \right)^{\frac{d-1}{d+1}}. \quad (6.59)$$

Since condition ECO2 requires a redshift much larger than this at the ECO surface (eq. (2.16)), we conclude that we again do not find an acceptable solution to the approximate TOV equation (6.26).

6.3 Checking the consistency of condition ECO3

The goal of condition ECO3 was to exclude situations where there is a significant amount of matter outside the radius R_{ECO} ; having such matter would conflict with the notion that our object is ‘extremely compact’. But we have noted that there is a certain amount of stress energy outside R_{ECO} that is unavoidable, since this stress-energy results from the state of quantum fields at temperature $T_{\text{ECO}}(r)$ in the near-surface region. We should therefore check that the stress-energy of this thermal gas is low enough at $s \gtrsim s_c$ so that we can indeed require that the geometry in this region is close to the black hole geometry. In this section we will check that such is the case, using estimates from the analysis above.

For the ECO geometry (2.4), the metric coefficient $e^{2\beta(r)}$ is given by (eq. 2.26))

$$e^{-2\beta(r)} = 1 - \frac{\mu GM(r)}{r^{d-2}}, \quad (6.60)$$

with

$$M(r) = M - E_{\text{rad}}(r). \quad (6.61)$$

Here $E_{\text{rad}}(r)$ is the energy contributed by the radiation in the region $r < r' \lesssim 2r_0$, where (as in the above sections) we have truncated our thermal gas at a scale $2r_0$. Following the lines of the computation leading to (5.14) we have

$$E_{\text{rad}}(r) \sim \frac{r_0^{\frac{d-3}{2}}}{(r - r_0)^{\frac{d-1}{2}}}. \quad (6.62)$$

In the black hole metric we have

$$e^{-2\beta_{\text{H}}(r)} = 1 - \frac{\mu GM}{r^{d-2}}. \quad (6.63)$$

Then we have, (still assuming $r \lesssim 2r_0$)

$$\frac{e^{-2\beta(r)}}{e^{-2\beta_{\text{H}}(r)}} = 1 + \frac{\mu GE_{\text{rad}}(r)}{r^{d-2} - \mu GM} = 1 + \frac{\mu GE_{\text{rad}}(r)}{r^{d-2} - r_0^{d-2}} \approx 1 + \frac{\mu GE_{\text{rad}}(r)}{(d-2)r_0^{d-3}(r - r_0)}. \quad (6.64)$$

Using arguments similar to the ones leading to (5.14) to estimate $E_{\text{rad}}(r)$, we find

$$\frac{\mu GE_{\text{rad}}(r)}{(d-2)r_0^{d-3}(r - r_0)} \sim \frac{l_p^{d-1}}{r_0^{\frac{d-3}{2}}(r - r_0)^{\frac{d+1}{2}}}. \quad (6.65)$$

For the ECO geometry to approximate the black hole geometry we need that the above quantity be $\lesssim 1$. This yields the requirement which is

$$(r - r_0) \gtrsim \left(\frac{l_p^{d-1}}{r_0^{\frac{d-3}{2}}} \right)^{\frac{2}{d+1}}. \quad (6.66)$$

From (6.37),(6.38) we see that this is just the condition $s \gtrsim s_c$. Thus the coefficient of g_{rr} in the ECO geometry satisfies the constraint ECO3.

The coefficient $\alpha(r)$ in the ECO geometry (2.4) is given through the equation

$$\frac{(d-1)\alpha'(r)e^{-2\beta(r)}}{r} = -\frac{(d-1)(d-2)(e^{-2\beta(r)}-1)}{2r^2} + 8\pi G p(r). \quad (6.67)$$

Using (2.26), this is

$$\frac{(d-1)\alpha'(r)e^{-2\beta(r)}}{r} = \frac{(d-1)(d-2)\mu GM(r)}{2r^d} + 8\pi G p(r). \quad (6.68)$$

For the black hole, we have (i) $e^{-2\beta_H(r)} = 1 - \frac{\mu GM}{r_0^{d-2}}$, (ii) $M(r) = M$, and (iii) $p = 0$. Then we get

$$\alpha'_H(r) = \frac{(d-2)\mu GM}{2r^{d-1}(1 - \frac{\mu GM}{r^{d-2}})}, \quad (6.69)$$

which gives

$$e^{2\alpha_H(r)} = 1 - \frac{\mu GM}{r^{d-2}}. \quad (6.70)$$

From the discussion above we have seen that $e^{-2\beta(r)}$ can be approximated by its black hole value for $s \gtrsim s_c$. On the RHS, again using estimates for E_{rad} similar to the one in (5.14), we find that for $s \gtrsim s_c$,

$$1 - \frac{M(r)}{M} = \frac{E_{rad}(r)}{M} \sim \frac{l_p^{d-1}}{r_0^{\frac{d-1}{2}}(r - r_0)^{\frac{d-1}{2}}} \sim \frac{l_p^{d-1}}{s^{d-1}} \lesssim \frac{l_p^{d-1}}{s_c^{d-1}} \sim \left(\frac{l_p}{r_0}\right)^{\frac{2(d-1)}{d+1}} \ll 1. \quad (6.71)$$

Thus in the first term on the RHS of (6.68) we can write $M(r) \approx M$. To see if $\alpha(r) \approx \alpha_H(r)$, we just need to check that the last term on the RHS of (6.68) can be ignored compared to the first term on the RHS; i.e., we need

$$\frac{p(r)r^d}{M} \lesssim 1. \quad (6.72)$$

But using the analysis leading to (6.37), we find that this inequality holds for $s \gtrsim s_c$.

To summarize, the thermal energy of quantum fields in the region $s \gtrsim s_c$ is small enough that the geometry in this region can be approximated by the black hole geometry. In particular, in this region the redshift in the ECO geometry is of the same order as its value in the black hole geometry. Thus it is consistent to impose condition ECO3 in our definition of an ECO to disallow additional sources of stress-energy outside R_{ECO} .

6.4 Summary

Let us summarize the discussion of this section. In section 5 we had performed a heuristic analysis of the total stress-energy — vacuum plus radiation — in the near-surface region of an ECO. We found that if $s_{\text{ECO}} < s_c$, then the backreaction of this stress-energy leads to a singularity in the metric (2.4), in the semiclassical region $r > R_{\text{ECO}}$. The analysis required us to separately consider the cases $T_{\text{ECO}} < T_H$ and $T_{\text{ECO}} > T_H$, and led to the conclusion that the only allowed situation is the one with $T_{\text{ECO}} = T_H$, where the stress-energy in this near-surface region vanishes. This analysis was not completely self-consistent however, as we

used the metric of the “core” of the ECO to find the redshift in the near-surface region, and did not take into account the fact that this redshift would also be affected by the stress-energy outside the core. Since the redshift at a point determines the energy density of radiation at that point, our estimates were heuristic to the extent that they did not use a fully self-consistent redshift.

In the present section we remedied this difficulty by considering the TOV equation which describes the metric coupled self-consistently with the stress-tensor. We gave plausibility arguments for adopting the perfect fluid stress-tensor (6.9), (6.10). Eq. (6.15) links the energy density at a point with the redshift at that point, now in a self-consistent fashion. Again we found that there is no regular solution satisfying the properties required of an ECO, if $s_{\text{ECO}} < s_c$. The analysis splits into two cases, which correspond to negative and positive values of ρ ; thus these cases parallel the $T_{\text{ECO}} < T_{\text{H}}$ and $T_{\text{ECO}} > T_{\text{H}}$ cases of section 5. We conclude that the only situation with no singularity in the semiclassical region $r > R_{\text{ECO}}$ is the one with $\rho = p = 0$, which we identify with the situation $T_{\text{ECO}} = T_{\text{H}}$ following (3.25).

7 An ECO in 1+1 dimensional dilaton gravity

In our study of the near-surface dynamics of an ECO, an important role has been played by the contribution to the stress-tensor from the quantum vacuum near the ECO surface. In the analysis of section 6, we allowed the vacuum energy density $\rho^v(r)$ to be arbitrary, but used some heuristic arguments to assume the form (6.9),(6.10) for the overall form of the stress tensor. In this section we will consider the case of 1+1 dimensional dilaton gravity, coupled to massless scalars. In this setting we can compute the vacuum energy explicitly using the conformal anomaly, and thus get a set of self-consistent equations describing the region $r > R_{\text{ECO}}$. More precisely, there will be vacuum energy as well as radiation energy outside the ECO, and the vacuum energy will be consistent with the metric which results from these two energies.

7.1 The model

The CGHS model [43] describes the quantum dynamics of 1+1 dimensional dilaton gravity coupled to a set of massless scalars f_i . The action is

$$I_{\text{CGHS}} = \frac{1}{2\pi} \int d^2x \sqrt{-g} [e^{-2\phi} (R + 4(\nabla\phi)^2 + 4\lambda^2) - \sum_{i=1}^n \frac{1}{2} (\nabla f_i)^2]. \quad (7.1)$$

Integrating out the scalars f_i gives a Polyakov term in the effective action of the form $R\Box^{-1}R$. This nonlocal term can be cast in a local form using an auxiliary field ψ with action

$$I_1 = -\frac{\kappa}{2\pi} \int d^2x \sqrt{-g} \left(\frac{1}{2} (\nabla\psi)^2 + \psi R \right). \quad (7.2)$$

Here κ is related to the number of scalar fields by $\kappa = (n-24)/24$. The shift $n \rightarrow n-24$ is due to ghosts, and we will assume that $n > 24$ so that $\kappa > 0$. The dynamics of these coupled fields can be simplified if we modify the action by the addition of a term $I_2 = -\frac{\kappa}{2\pi} \int d^2x \sqrt{-g} \phi R$, which yields the RST model [44]. We then arrive at the action

$$I = -\frac{1}{2\pi} \int d^2x \sqrt{-g} \left[e^{-2\phi} (R + 4(\nabla\phi)^2 + 4\lambda^2) + \kappa \left(\frac{(\nabla\psi)^2}{2} + \psi R + \phi R \right) \right]. \quad (7.3)$$

Variation of the metric $g^{\mu\nu}$ gives

$$\frac{e^{-2\phi}}{\pi} \left(-2g_{\mu\nu}(\square\phi - (\nabla\phi)^2 + \lambda^2) + 2\nabla_\mu\nabla_\nu\phi \right) - \frac{\kappa}{2\pi} \left(\nabla_\mu\psi\nabla_\nu\psi - 2\nabla_\mu\nabla_\nu\psi - g_{\mu\nu}(-2R + \frac{1}{2}(\nabla\psi)^2) \right) - \frac{\kappa}{\pi}(g_{\mu\nu}\square\phi - \nabla_\mu\nabla_\nu\phi) = 0. \quad (7.4)$$

Variation of the dilaton ϕ gives

$$e^{-2\phi}(R - 4(\nabla\phi)^2 + 4\square\phi + 4\lambda^2) = -\kappa\frac{R}{2}, \quad (7.5)$$

and variation of the auxiliary field ψ gives

$$\square\psi = R. \quad (7.6)$$

Taking the trace of the metric equation, and using the other two field equations, we find

$$(R + 2\square\phi)(\frac{\kappa}{2} - e^{-2\phi}) = 0. \quad (7.7)$$

We are interested in the solution where ϕ is not a constant, which implies

$$R = -2\square\phi. \quad (7.8)$$

Combined this with (7.6) gives

$$\psi = -2\phi + w \implies \square w = 0. \quad (7.9)$$

7.2 Solving the equations

We wish to solve the above equations using a coordinate choice which is similar to the Schwarzschild type coordinates (2.4) that we used in higher dimensions. We list below key steps from the discussion of [25], where the above equations were nicely analyzed.

(i) We take the static ansatz

$$ds^2 = -\tilde{g}(x)dt^2 + \tilde{g}^{-1}(x)dx^2 = -g(\phi)dt^2 + g^{-1}(\phi)h^2(\phi)d\phi^2, \quad (7.10)$$

where in the second step we have used ϕ as a spatial coordinate in place of x , and $\tilde{g}(x) = g(\phi(x))$. At spatial infinity we will have flat spacetime, with curvature $R = 0$. From eq.(7.5) we find that $\phi = \pm\lambda x$ at infinity; we choose the solution $\phi = -\lambda x$. At $x \rightarrow \infty$ we will then get

$$\phi \rightarrow -\infty, \quad g(\phi) \rightarrow 1, \quad h(\phi) \rightarrow -\frac{1}{\lambda}. \quad (7.11)$$

For the above static metric, the equation $\square w = 0$ (7.9) can be solved:

$$\partial_x w(x) = \frac{C}{\tilde{g}(x)} \implies \partial_\phi w(\phi) \equiv w' = C \frac{h(\phi)}{g(\phi)}, \quad (7.12)$$

where C is an integration constant, and primes denote derivatives with respect to ϕ .

(ii) In the metric (7.10), the $\phi\phi$ component of the metric equation (7.4) gives, after some algebra

$$\left(1 - \frac{\kappa}{2}e^{2\phi}\right) \frac{h'(\phi)}{h(\phi)} = -\kappa e^{2\phi} \left(\left(1 - \frac{Ch(\phi)}{2g(\phi)}\right)^2 + \frac{C}{2} \frac{g'(\phi)h(\phi)}{(g(\phi))^2} \right). \quad (7.13)$$

The dilaton equation (7.5) gives

$$-\left(1 - \frac{\kappa}{2}e^{2\phi}\right) \left(\frac{h'(\phi)}{h(\phi)} - \frac{g'(\phi)}{g(\phi)}\right) - 2 + 2\lambda^2 \frac{(h(\phi))^2}{g(\phi)} = 0. \quad (7.14)$$

For the static metric (7.10), $R = \partial_x^2 \tilde{g}(x)$. Converting derivatives in ∂_x to derivatives $\partial_\phi = h\partial_x$, the equation $R = -2\Box\phi$ can be integrated to give

$$g'(\phi) = 2g(\phi) - d_\lambda h(\phi), \quad (7.15)$$

where d_λ is an integration constant. Eq. (7.15) can be solved by introducing a new function $Z(\phi)$,

$$g(\phi) = -\frac{d_\lambda}{2\lambda} e^{2\phi} Z(\phi), \quad h(\phi) = e^{2\phi} \frac{Z'(\phi)}{2\lambda}. \quad (7.16)$$

The limit (7.11) gives

$$d_\lambda = -2\lambda. \quad (7.17)$$

so that we have

$$g(\phi) = e^{2\phi} Z(\phi), \quad h(\phi) = e^{2\phi} \frac{Z'(\phi)}{2\lambda}. \quad (7.18)$$

(iii) In the dilaton equation (7.14) we note that $\frac{g'}{g} - \frac{h'}{h} = \frac{h}{g} \left(\frac{g}{h}\right)'$. Then (7.14) becomes

$$\left(\left(e^{-2\phi} - \frac{\kappa}{2}\right) \left(\frac{g}{h}\right)\right)' = -2\lambda^2 h e^{-2\phi} = -\lambda Z', \quad (7.19)$$

which can be integrated to yield

$$g(\phi) = \frac{2\lambda h(\phi) e^{2\phi}}{\kappa e^{2\phi} - 2} (Z(\phi) + A_C), \quad (7.20)$$

where A_C is an integration constant. Substituting in this relation the expressions (7.18) for $g(\phi)$ and $h(\phi)$, we get an equation for $Z(\phi)$ which is easily integrated to give

$$Z(\phi) + A_C \ln Z(\phi) = \kappa\phi + e^{-2\phi} + a_1, \quad (7.21)$$

where a_1 is another integration constant.

(iv) We must now relate the constant A_C to the integration constant C that we had introduced earlier in (7.12). In the metric equation (7.13) we can replace $\frac{h'}{h}$ from (7.14) and then replace any derivatives g' using (7.15). This gives

$$2\lambda^2 \frac{h^2}{g} + \frac{2\lambda h}{g} - \frac{\lambda h}{g} \kappa e^{2\phi} = -\frac{C}{2} \left(\frac{C}{2} + 2\lambda\right) \frac{h^2}{g^2} \kappa e^{2\phi}. \quad (7.22)$$

Using the forms (7.18) for g and h , this gives

$$e^{2\phi} \frac{(Z')^2}{2Z} + \frac{Z'}{Z} - \frac{Z'}{Z} \frac{\kappa}{2} e^{2\phi} = -\frac{C}{2} \left(\frac{C}{2} + 2\lambda \right) \frac{(Z')^2}{4\lambda^2 Z^2} \kappa e^{2\phi}. \quad (7.23)$$

Also, using the forms (7.18) for g and h in (7.20) gives

$$Z' = \frac{Ze^{-2\phi}}{Z + A_C} (\kappa e^{2\phi} - 2). \quad (7.24)$$

Using this in (7.23) gives

$$-\frac{e^{-2\phi} (\kappa e^{2\phi} - 2)^2 (-8A_C \lambda^2 + C^2 \kappa + 4C\kappa\lambda)}{16\lambda^2 (A_C + Z)^2} = 0, \quad (7.25)$$

from which we read off

$$A_C = \frac{\kappa}{8\lambda^2} C(C + 4\lambda).$$

(v) Summarizing the above steps, we find that the complete solution of our coupled equations is given in terms of one integration constant C , in the form

$$g(\phi) = e^{2\phi} Z(\phi), \quad h(\phi) = \frac{1}{2\lambda} e^{2\phi} Z'(\phi), \quad (7.26)$$

where $Z(\phi)$ is found by solving the equation

$$Z(\phi) + A_C \ln \left(\frac{Z(\phi)}{|A_C|} \right) = e^{-2\phi} + \kappa\phi - a_2, \quad A_C = \frac{\kappa}{8\lambda^2} C(C + 4\lambda), \quad (7.27)$$

where we have written $a_2 = -a_1 + A_C \log |A_C|$.

7.3 Finding the Boulware and Hartle-Hawking states

The integration constant C determines the different quantum states of the matter fields on our spacetime through their contribution to the stress-tensor at infinity. Recall that we have integrated out the matter fields to obtain a nonlocal Polyakov which has then been rewritten in terms of the auxiliary field ψ , giving the action (7.2). Varying $g^{\mu\nu}$ in this action gives the stress tensor

$$T_{\mu\nu}^{(1)} = -\frac{\kappa}{2\pi} \left(\nabla_\mu \psi \nabla_\nu \psi - 2\nabla_\mu \nabla_\nu \psi - g_{\mu\nu} \left(-2R + \frac{1}{2} (\nabla\psi)^2 \right) \right). \quad (7.28)$$

Using the metric (7.10) to compute covariant derivatives, and using the relations $\psi = -2\phi + w$ and $w' = \frac{Ch}{g}$, we get

$$T_t^{(1)t} = -\frac{\kappa}{2\pi} \left(\frac{6g}{h^2} + \frac{4\lambda}{h} + \frac{C(C + 4\lambda)}{2g} - \frac{4gh'}{h^3} \right). \quad (7.29)$$

At $x \rightarrow \infty$, we have the limit (7.11), which yields

$$\rho(x = \infty) = -T_t^{(1)t}(x = \infty) = \frac{\kappa}{4\pi} (C + 2\lambda)^2. \quad (7.30)$$

The Boulware vacuum corresponds to the case of no energy density at infinity, so we need $T_t^{(1)t}(x = \infty) = 0$. This gives

$$C = -2\lambda. \quad (7.31)$$

In the Hartle-Hawking vacuum we need smoothness at the horizon. This implies a finite value of the energy density at the horizon where $g \rightarrow 0$. In (7.29) we see that the third term on the RHS diverges as $g \rightarrow 0$, unless

$$C = 0 \quad \text{or} \quad C = -4\lambda. \quad (7.32)$$

Thus these two values of C describe the Hartle-Hawking vacuum. With the values of C in (7.32), we have $A_C = 0$. The horizon corresponds to the point where $g_{tt} = -g(\phi) = 0$, which from (7.26) implies $Z = 0$. From (7.27), we see that the horizon is at $\phi = \phi_0$ where

$$e^{-2\phi_0} + \kappa\phi_0 - a_2 = 0, \quad (7.33)$$

We define

$$M = \frac{\lambda a_2}{\pi}, \quad (7.34)$$

as the mass of the hole.

7.4 Analysis of the solution

With the above solution of 1+1 dimensional gravity coupled to scalars, we can now address the temperature of an ECO. Let T_H be the temperature of the black hole and thus the temperature at infinity of the Hartle-Hawking vacuum. Putting the values of C from (7.32) into (7.30) we find that the energy density at infinity of the Hartle-Hawking vacuum is $\rho_{HH}(\infty) = \frac{\kappa\lambda^2}{\pi}$. For $T_{\text{ECO}} < T_H$, the energy density at infinity should be less than $\rho_{HH}(\infty)$, which implies $-4\lambda < C < 0$. For this range of C , we have $A_C < 0$. Conversely, for $T_{\text{ECO}} > T_H$, we need $C < -4\lambda$ or $C > 0$; in these cases we have $A_C > 0$.

Note that the radius of the black hole can be considered to be $r_0 \equiv e^{-\phi_0}$ and since we are interested in a large black hole, we will take

$$\phi_0 \ll 0. \quad (7.35)$$

Thus $|\phi_0| \ll e^{-\phi_0}$; we can use this to simplify our qualitative understanding of the solution of (7.27).

Let us now consider the cases $T_{\text{ECO}} < T_H$ and $T_{\text{ECO}} > T_H$ in turn.

7.4.1 $T_{\text{ECO}} < T_H$

In this case $A_C < 0$, so we write $A_C = -|A_C|$. For $\frac{(T_H - T_{\text{ECO}})}{T_H} \sim 1$, we have $|A_C| \sim \kappa$. We will assume $\kappa \sim 1$ in what follows, and thus take $|A_C| \sim 1$.

At spatial infinity, we have $\phi \rightarrow -\infty$, and from (7.27) we have $Z \sim e^{-2\phi}$. Let us move inwards from infinity, which implies that we move towards larger values of ϕ , and look for the first point where we have a difficulty with the solution of (7.27). Differentiating this equation we find

$$Z' = \frac{(\kappa - 2e^{-2\phi})}{(1 - \frac{|A_C|}{Z})}. \quad (7.36)$$

Thus the solution fails when we reach $Z = |A_C|$. From (7.27) we see that this value of Z corresponds to a point $\phi_* > \phi_0$. Using (7.33) we find

$$\Delta\phi \equiv (\phi_* - \phi_0) \approx -\frac{|A_C|}{2} e^{2\phi_0}. \quad (7.37)$$

Since $\phi_0 \ll 0$ for a large black hole, we see that $|\Delta\phi|$ is very small. At $\phi = \phi_*$ we find that

$$g(\phi_*) = Z(\phi_*) e^{2\phi_*} \approx \frac{|A_C|}{2} e^{2\phi_0}. \quad (7.38)$$

Thus the redshift parameter at ϕ_* is

$$q(\phi_*) \equiv (-g_{tt}(\phi_*))^{-\frac{1}{2}} = (g(\phi_*))^{-\frac{1}{2}} \approx \left(\frac{2}{|A_C|}\right)^{\frac{1}{2}} e^{-\phi_0}. \quad (7.39)$$

Again noting that $\phi_0 \ll 0$, we have $q(\phi_*) \gg 1$.

Let us now try to place this solution in the context of an ECO. Since the solution fails at $\phi = \phi_*$, we should place a surface just outside this point, at a location we call ϕ_{ECO} with $\phi_{\text{ECO}} < \phi_*$. We then imagine that some other quantum gravitational dynamics takes over in the region $\phi > \phi_{\text{ECO}}$. Of course we have already solved the full quantum gravity dynamics arising from the action (7.3), with the solution given in (7.27). Thus to get some novel dynamics at $\phi > \phi_{\text{ECO}}$, we must imagine that there are other quantum fields in the complete theory. These fields can be, for example, fields with large mass that do not contribute significantly to the action at $\phi \ll 0$, but which can still modify the dynamics to something that is regular at $\phi > \phi_{\text{ECO}}$. Such a picture brings the problem to the same footing as our analysis of the situation in higher dimensions d .

We can now see qualitative similarities between what we have found above and the situation for higher d . Since we must take $\phi_{\text{ECO}} < \phi_*$, we find that the redshift at the ECO surface ϕ_{ECO} is bounded as

$$q(\phi_{\text{ECO}}) < \left(\frac{2}{|A_C|}\right)^{\frac{1}{2}} e^{-\phi_0}. \quad (7.40)$$

Thus we cannot have an ECO for $T_{\text{ECO}} < T_{\text{H}}$ if we demand that the redshift at the ECO surface is higher than the value in the RHS of (7.40). Note that this maximum redshift is finite but large, since $\phi_0 \ll 0$.

We cannot make a more precise comparison to the situation for higher d since we do not have any simple way to extrapolate expressions like (1.5) to the case $d = 1$. This difficulty is already present at the classical level. For $d > 2$, the radius of the hole grows with its mass as $r_0 \sim M^{\frac{1}{d-2}}$. Extrapolating this expression to $d = 1$ would suggest $r_0 \sim M^{-1}$, which would indicate a radius that goes down as the mass increases. But from (7.34) we expect that even for the case $d = 1$, a larger M implies a larger radius $r_0 \equiv e^{-\phi_0}$. We will find further differences between the cases of $d = 1$ and higher d below.

7.4.2 $T_{\text{ECO}} > T_{\text{H}}$

In this case $A_C > 0$, so we write $A_C = |A_C|$ for clarity. Again, for $\frac{(T_{\text{ECO}} - T_{\text{H}})}{T_{\text{H}}} \sim 1$, we have $|A_C| \sim \kappa$. As in the above subsection, we will assume $\kappa \sim 1$ in what follows, and thus take $|A_C| \sim 1$.

This time the analogue of (7.36) is

$$Z' = \frac{\kappa - 2e^{-2\phi}}{1 + \frac{|A_C|}{Z}}. \quad (7.41)$$

We have $Z > 0$ throughout our analysis, since g would become singular at $Z = 0$. The denominator is thus regular for all Z . But the numerator vanishes at

$$\phi_s = -\frac{1}{2} \ln \frac{\kappa}{2}. \quad (7.42)$$

We see that ϕ_s is a number of order unity, and thus describes the ‘strong coupling’ region of dilaton gravity. This location can be considered to be the analogue of $r_s \sim l_p$ in higher dimensions. We are not interested in looking at the analogue of a central singularity at $r = 0$, but at the behavior near the horizon location $\phi = \phi_0$. While we do not have a singularity in the solution at $\phi \approx \phi_0$, there is an interesting change of behavior as we pass this location, which we now note.

For $\phi < \phi_0$, the RHS of (7.27) is positive. At $\phi = \phi_0$, the RHS vanishes. For

$$\phi_s \ll \phi \lesssim \phi_0, \quad (7.43)$$

the RHS becomes $\approx -a \sim -e^{-2\phi_0}$ (we have used $\phi_0 \ll 0$ to drop terms like ϕ_0 compared to exponentials $e^{-2\phi_0}$). This large negative value is reproduced on the LHS by a very small (positive) value of Z . The first term Z on the LHS becomes ignorable, and we are left with

$$|A_C| \ln \frac{Z}{|A_C|} \approx -e^{-2\phi_0}, \quad (7.44)$$

which gives (using $|A_C| \sim 1$)

$$Z \sim e^{-e^{-2\phi_0}}, \quad (7.45)$$

which is a very tiny number. From this we find that in the region (7.43)

$$g(\phi) \sim e^{-e^{-2\phi_0}} e^{2\phi_0}. \quad (7.46)$$

The second factor on the RHS is a small correction to the first factor, and not relevant by itself in the approximation in which we have written (7.45), but we keep this factor in g since we will be comparing g to h below, and the ratio will involve this subleading factor. We also have

$$Z' = \frac{(\kappa - 2e^{-2\phi})}{(1 + \frac{|A_C|}{Z})} \approx -\frac{2}{|A_C|} e^{-2\phi_0} Z, \quad (7.47)$$

and

$$h(\phi) = \frac{1}{2\lambda} e^{2\phi} Z'(\phi) \approx \frac{1}{2\lambda} e^{2\phi_0} Z'(\phi) \approx -\frac{1}{2\lambda} \frac{2}{|A_C|} Z \sim -\frac{1}{\lambda} e^{-e^{-2\phi_0}}. \quad (7.48)$$

Thus in the metric (7.10), in the region (7.43), the coefficient of $-dt^2$ and $d\phi^2$ are both very small due to the factor $Exp[-e^{-2\phi_0}]$. Note however that

$$\frac{g}{\lambda h} \sim e^{2\phi_0} \ll 1. \quad (7.49)$$

Suppose one were to put a surface at some point ϕ_{ECO} in the region (7.43) and replace its interior by some new physics. Then this object would satisfy the spirit of condition ECO1 since $\phi_{\text{ECO}} > \phi_0$ (i.e. the ECO surface is *inside* the horizon radius). The redshift parameter at this surface is

$$q(\phi_{\text{ECO}}) \equiv (-g_{tt}(\phi_{\text{ECO}}))^{-\frac{1}{2}} \sim e^{\frac{1}{2}e^{-2\phi_0}}, \quad (7.50)$$

which cannot be made arbitrarily large, but must still be considered extremely large since $\phi_0 \ll 0$. Thus in a rough sense one could say that this looks like an ECO, with $T_{\text{ECO}} > T_{\text{H}}$. We can see how this situation escaped our earlier arguments against such an ECO in higher dimensions. On the RHS of eq.(6.31), for example, we have the power $\frac{2d}{d-1}$ which is a finite positive number for $d > 1$, but diverges for $d = 1$. A similar singularity $\sim \frac{1}{d-1}$ in a power is encountered in other relations like (6.46), (6.53). Thus our general analysis does not work for the case $d = 1$, and we may have an ECO like object with $T_{\text{ECO}} > T_{\text{H}}$.

7.5 The form of the stress tensor

Recall that in section 6 we had given arguments as to why the vacuum stress tensor could be taken to be traceless to leading order in the high redshift region near the surface of an ECO. This had led to a traceless form of the total stress energy (eq.(6.9)), (6.10). In the present case of $d = 1$, we have the exact stress energy from our solution, so we can check if such a traceless condition is indeed maintained.

In the case of $T_{\text{ECO}} < T_{\text{H}}$ studied in section 7.4.1, the solution becomes singular outside the horizon radius, so we cannot approach closer than to the horizon than the distance $|\Delta\phi|$ given in (7.37). But in the case $T_{\text{ECO}} > T_{\text{H}}$ studied in section 7.4.2, the solution continues past the horizon location $\phi = \phi_0$. Thus we can investigate if the condition $p \approx \rho$ holds in the region near the horizon in the exact analysis of the $d = 1$ case.

From the stress tensor (7.28) we find

$$T_x^{(1)x} = p = \frac{\kappa}{2\pi} \left(\frac{28g}{h^2} + \frac{24\lambda}{h} + \frac{C(C+4\lambda)}{2g} - \frac{16gh'}{h^3} \right), \quad (7.51)$$

and

$$-T_t^{(1)t} = \rho = \frac{\kappa}{2\pi} \left(\frac{6g}{h^2} + \frac{4\lambda}{h} + \frac{C(C+4\lambda)}{2g} - \frac{4gh'}{h^3} \right). \quad (7.52)$$

We are interested in the relation between ρ and p in the horizon region $\phi \approx \phi_0$, where the coefficients of the metric change very sharply. In this region we find that both g and h become very small, but as noted in (7.49), g is smaller than λh by a factor $\sim e^{2\phi_0}$. We also need to estimate

$$\begin{aligned} h' &= \frac{1}{2\lambda} e^{2\phi} Z''(\phi) + \frac{1}{\lambda} \frac{(\kappa e^{2\phi} - 2)}{1 + \frac{|A_C|}{Z}}, \\ &= \frac{\kappa}{\lambda} \frac{e^{2\phi}}{1 + \frac{|A_C|}{Z}} + \frac{1}{2\lambda} \frac{(\kappa e^{2\phi} - 2)}{(1 + \frac{|A_C|}{Z})^2} \frac{|A_C|}{Z^2} Z', \\ &\approx \frac{\kappa}{\lambda |A_C|} e^{2\phi_0} Z + \frac{2}{\lambda |A_C|^2} e^{-2\phi_0} Z, \\ &\approx \frac{2}{\lambda |A_C|^2} e^{-2\phi_0} Z. \end{aligned} \quad (7.53)$$

Using (7.45) and (7.46), we find that

$$\frac{\lambda h'}{g} \sim e^{-4\phi_0}. \quad (7.54)$$

Using (7.49),(7.54) in (7.51) and (7.52), we find that in each case one term dominates over the other terms giving

$$p \approx \frac{\kappa}{2\pi} \frac{C(C+4\lambda)}{2g}, \quad (7.55)$$

and

$$\rho \approx \frac{\kappa}{2\pi} \frac{C(C+4\lambda)}{2g}. \quad (7.56)$$

Thus we find that $p \approx \rho$ near the horizon radius ϕ_0 .

8 Discussion

In this paper we have argued that Extremely Compact Objects (ECOs) must have the same thermodynamic properties — temperature T , entropy S and radiation rates $\Gamma[\{l\}, \omega]$ — as a semiclassical black hole of the same mass.

This result is relevant for the following reason. The semiclassical hole has an appealing thermodynamics, which seems to be related to the existence of a horizon. But a horizon leads to a loss of quantum unitarity in the process of black hole evaporation. In string theory we find that black hole microstates are fuzzballs with no horizon. This resolves the information puzzle, but leaves us with a different question: if fuzzballs have no horizon, then is there any reason to expect that they reproduce the thermodynamic properties of the semiclassical hole?

Entropic arguments suggest that fuzzballs have a surface that is at a distance $s \sim l_p$ outside the horizon radius. ECOs have also been postulated in many other theories of gravity (for a discussion, see for example [20]). We have found that if the ECO surface is at a distance $s_{\text{ECO}} \ll (M/m_p)^{\frac{2}{(d-2)(d+1)}}$ from the horizon radius r_0 , then the temperature T_{ECO} must agree with the Hawking temperature T_H , to an accuracy which improves as s is made smaller. The central aspect of the argument involved studying the Tolman-Oppenheimer-Volkoff equation in the near surface approximation. This near-surface region is filled with a gas of radiation, whose temperature and energy density are very high due to the large redshift at the ECO surface. A negative contribution to the energy density comes from the vacuum ‘Casimir’ energy, which we argued must be the same to leading order as the negative energy density of the local Rindler vacuum. We find that if the sum of radiation and vacuum energies does not vanish, then the back-reaction of the near energy density on the geometry does not allow for a consistent time-independent solution. The two sources of energy cancel for $T_{\text{ECO}} = T_H$, giving the agreement of temperatures mentioned above.

Once we have an agreement of temperatures between the ECO and the black hole, the agreement of entropies follows from standard thermodynamics. The agreement of radiation rates is due to the large redshift at the ECO surface. This redshift separates the thermal bath near the ECO surface from the region where the quanta must penetrate an effective potential to emerge at infinity. This separation leading to an agreement of graybody factors with the semiclassical hole once we are given an agreement of temperatures.

Thus these results provide a satisfying closure to the fuzzball paradigm of black holes. The information paradox is resolved because no microstate has a horizon. But the elegant thermodynamics emerging from the semiclassical hole is still preserved, due to the agreements of temperature, entropy, radiation rates.

We have not studied the dynamical processes which would bring an ECO to a temperature $T_{\text{ECO}} = T_{\text{H}}$ if we initially start with an object with $T \neq T_{\text{H}}$. But qualitatively, we envisage the following. If $T > T_{\text{H}}$, then the quantum structure at $r < R_{\text{ECO}}$ will grow in size by absorbing the high temperature radiation near the object's surface, until the temperature just outside this surface drops to a value which equals the Hawking temperature, and a time-independent ECO can exist. Conversely, if $T < T_{\text{H}}$, then the quantum structure near the surface will shrink, giving up its energy to heat the radiation near the surface; equilibrium will be reached when the temperature of this radiation equals T_{H} , allowing an ECO to exist.

Our analysis suggests several avenues for future work. We defined $\eta_T = T_{\text{ECO}}/T_{\text{H}}$, and argued that if $\eta_T \neq 1$, then there would be no consistent solution to the near-surface Einstein equations. But $\Delta T \equiv T_{\text{ECO}} - T_{\text{H}}$ could still be nonzero and parametrically smaller than T_{H} . It would be interesting to work out how the allowed range ΔT goes to zero as s_{ECO} goes towards smaller values.

It is possible to get a completely self-consistent solution of the quantum field equations in the 1+1 dimensional case. We have noted qualitative similarities between this case and the situation in higher dimensions, though there were some differences as well due to a divergence $\sim \frac{1}{d-1}$ in the power law behavior of quantities in the Tolman-Oppenheimer-Volkoff equation.

It would also be interesting to extend the present analysis for black holes with charge and rotation, particularly as we go towards charge and rotation values that are extremal.

Acknowledgments

This work is supported in part by DOE grant DE-SC0011726. We would like to thank for discussions Iosif Bena, Robert Brandenberger, Marcel Hughes, Pierre Heidmann, Brandon Manley, Ted Jacobson, Juan Maldacena, Robert Mann, Geoff Penington and Nicholas Warner.

References

- [1] S. W. Hawking. Particle Creation by Black Holes. *Commun. Math. Phys.*, 43:199–220, 1975.
- [2] Jacob D. Bekenstein. Black holes and entropy. *Phys. Rev. D*, 7:2333–2346, Apr 1973.
- [3] S. W. Hawking. Breakdown of Predictability in Gravitational Collapse. *Phys. Rev. D*, 14:2460–2473, 1976.
- [4] Samir D. Mathur. The Information paradox: A Pedagogical introduction. *Class. Quant. Grav.*, 26:224001, 2009.
- [5] Oleg Lunin and Samir D. Mathur. AdS / CFT duality and the black hole information paradox. *Nucl. Phys. B*, 623:342–394, 2002.

- [6] Oleg Lunin, Juan Martin Maldacena, and Liat Maoz. Gravity solutions for the D1-D5 system with angular momentum. 12 2002.
- [7] Ingmar Kanitscheider, Kostas Skenderis, and Marika Taylor. Fuzzballs with internal excitations. *JHEP*, 06:056, 2007.
- [8] Samir D. Mathur. The Fuzzball proposal for black holes: An Elementary review. *Fortsch. Phys.*, 53:793–827, 2005.
- [9] Iosif Bena and Nicholas P. Warner. Black holes, black rings and their microstates. *Lect. Notes Phys.*, 755:1–92, 2008.
- [10] Borun D. Chowdhury and Amitabh Virmani. Modave Lectures on Fuzzballs and Emission from the D1-D5 System. In *5th Modave Summer School in Mathematical Physics*, 1 2010.
- [11] Iosif Bena, Stefano Giusto, Rodolfo Russo, Masaki Shigemori, and Nicholas P. Warner. Habemus Superstratum! A constructive proof of the existence of superstrata. *JHEP*, 05:110, 2015.
- [12] Iosif Bena, Stefano Giusto, Emil J. Martinec, Rodolfo Russo, Masaki Shigemori, David Turton, and Nicholas P. Warner. Smooth horizonless geometries deep inside the black-hole regime. *Phys. Rev. Lett.*, 117(20):201601, 2016.
- [13] Samir D. Mathur. The VECRO hypothesis. 1 2020.
- [14] Iosif Bena, Emil J. Martinec, Samir D. Mathur, and Nicholas P. Warner. Fuzzballs and Microstate Geometries: Black-Hole Structure in String Theory. 4 2022.
- [15] Bin Guo, Shaun Hampton, and Samir D. Mathur. Can we observe fuzzballs or firewalls? *JHEP*, 07:162, 2018.
- [16] Samir D. Mathur and Madhur Mehta. The universality of black hole thermodynamics. *Int. J. Mod. Phys. D*, 32(14):2341003, 2023.
- [17] F. Pretorius, D. Vollick, and W. Israel. An Operational approach to black hole entropy. *Phys. Rev. D*, 57:6311–6316, 1998.
- [18] Shinji Mukohyama and Werner Israel. Black holes, brick walls and the Boulware state. *Phys. Rev. D*, 58:104005, 1998.
- [19] Gerard 't Hooft. On the Quantum Structure of a Black Hole. *Nucl. Phys. B*, 256:727–745, 1985.
- [20] Vitor Cardoso and Paolo Pani. Testing the nature of dark compact objects: a status report. *Living Rev. Rel.*, 22(1):4, 2019.
- [21] Robert B. Mann, Sebastian Murk, and Daniel R. Terno. Black holes and their horizons in semiclassical and modified theories of gravity. *Int. J. Mod. Phys. D*, 31(09):2230015, 2022.
- [22] Ram Brustein, A. J. M. Medved, and Tamar Simhon. Thermodynamics of frozen stars. 10 2023.

[23] Wan Zhen Chua and Niayesh Afshordi. Electromagnetic albedo of quantum black holes. *Journal of High Energy Physics*, 2021(7), July 2021.

[24] Yuan Yue and Yong-Qiang Wang. Frozen hayward-boson stars, 2023.

[25] Yohan Potaux, Debajyoti Sarkar, and Sergey N. Solodukhin. Quantum states and their back-reacted geometries in 2d dilaton gravity. *Phys. Rev. D*, 105:025015, Jan 2022.

[26] H. A. Buchdahl. General relativistic fluid spheres. *Phys. Rev.*, 116:1027–1034, Nov 1959.

[27] Samir D. Mathur. What prevents gravitational collapse in string theory? *Int. J. Mod. Phys. D*, 25(12):1644018, 2016.

[28] Ibrahima Bah, Pierre Heidmann, and Peter Weck. Schwarzschild-like topological solitons. *JHEP*, 08:269, 2022.

[29] Pierre Heidmann. Non-BPS floating branes and bubbling geometries. *JHEP*, 02:162, 2022.

[30] Pierre Heidmann and Madhur Mehta. Electromagnetic Entrapment in Gravity. 12 2023.

[31] Pierre Heidmann. Half the Schwarzschild Entropy From Strominger and Vafa. 12 2023.

[32] Ibrahima Bah and Pierre Heidmann. Geometric Resolution of Schwarzschild Horizon. 3 2023.

[33] P. Candelas. Vacuum Polarization in Schwarzschild Space-Time. *Phys. Rev. D*, 21:2185–2202, 1980.

[34] W. G. Unruh. Notes on black hole evaporation. *Phys. Rev. D*, 14:870, 1976.

[35] David G. Boulware. Quantum Field Theory in Schwarzschild and Rindler Spaces. *Phys. Rev. D*, 11:1404, 1975.

[36] J. B. Hartle and S. W. Hawking. Path Integral Derivation of Black Hole Radiance. *Phys. Rev. D*, 13:2188–2203, 1976.

[37] S. M. Christensen. Vacuum Expectation Value of the Stress Tensor in an Arbitrary Curved Background: The Covariant Point Separation Method. *Phys. Rev. D*, 14:2490–2501, 1976.

[38] S. A. Fulling. Alternative Vacuum States in Static Space-Times with Horizons. *J. Phys. A*, 10:917–951, 1977.

[39] S. M. Christensen and S. A. Fulling. Trace Anomalies and the Hawking Effect. *Phys. Rev. D*, 15:2088–2104, 1977.

[40] G. W. Gibbons and S. W. Hawking. Action integrals and partition functions in quantum gravity. *Phys. Rev. D*, 15:2752–2756, May 1977.

[41] N. D. Birrell and P. C. W. Davies. *Quantum Fields in Curved Space*. Cambridge Monographs on Mathematical Physics. Cambridge Univ. Press, Cambridge, UK, 2 1984.

- [42] S. Chandrasekhar. *An Introduction to the Study of Stellar Structure* . Dover Publications, Cambridge, UK, 1975.
- [43] Curtis G. Callan, Steven B. Giddings, Jeffrey A. Harvey, and Andrew Strominger. Evanescent black holes. *Phys. Rev. D*, 45:R1005–R1009, Feb 1992.
- [44] Jorge G. Russo, Leonard Susskind, and Lárus Thorlacius. End point of hawking radiation. *Phys. Rev. D*, 46:3444–3449, Oct 1992.